

# Recent advances in the NMR of fuel: a brief overview

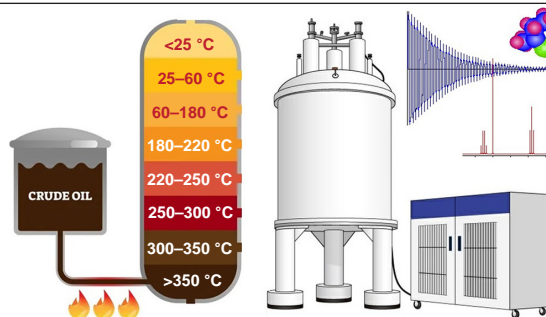
Leonid B. Krivdin 

*A.E.Favorsky Irkutsk Institute of Chemistry, Siberian Branch of the Russian Academy of Sciences,  
ul. Favorskogo 1, 664033 Irkutsk, Russian Federation*

Present review covers the most recent advances in the NMR studies of oil refining products — light fractions, different types of fuels, heavy fractions, and crude oil itself. By no means does it discuss NMR applications in this field in detail providing only a brief overview of different NMR methods used for the structural elucidation of the oil refining products together with crude oil with particular emphasis on recent achievements and advances in this field.

The bibliography includes 48 references.

**Keywords:** NMR, fuel, light fractions, coker naphtha, heavy fractions, asphaltenes, crude oil.



## Contents

1. Introduction	1
2. NMR of fuel: recent advances and perspectives	2
2.1. Light fractions	2
2.2. Fuels	5
2.3. Asphaltenes	9
2.4. Crude oil	11
3. Conclusion	19
4. Abbreviations	21
5. References	21

*This review is dedicated to late Professor Dmitry Filippovich Kushnarev, one of the pioneers of this field in Russia. The achievements of the Department of Analytical Chemistry at the University of Irkutsk headed by late Professor D.F.Kushnarev are inextricably connected with the Irkutsk scientific school 'Quantitative NMR spectroscopy of natural organic raw materials — oil, coal, and wood', which was founded in 1972 by Professor G.A.Kalabin and continued later by Professor D.F.Kushnarev. The results in this field gained by Irkutsk scientists were published in 7 monographs and more than 400 papers, and also presented in 7 DSc and 28 PhD dissertations. One of the well-known monographs in this area is the book by G.A.Kalabin, L.V.Kanitskaya, and D.F.Kushnarev 'Quantitative NMR Spectroscopy of Natural Organic Raw Materials and its Processing Products'.*

**L.B.Krivdin** graduated from M.V.Lomonosov Moscow State University in 1977, received his PhD in 1982 from the Irkutsk State University, which was followed by a postdoctoral fellowship at Flinders University of South Australia in the group of Professor Ernst Della (1990–1991). He received his DSc in 1989 and Full Professor in 1993. His research interests focus on computation of NMR parameters being substantiated with some 400 research publications, including approximately 20 reviews and book chapters. Under his scientific supervision, 12 PhD dissertations were defended in the interim of 1989 until present. Professor Krivdin visited 50 countries being invited as a visiting professor of a number of different universities involving those in Russia, the United States, Australia, Argentina, the United Kingdom, Poland, France and many others around the world. He is currently a Chief Researcher in the NMR Laboratory at A.E.Favorsky Irkutsk Institute of Chemistry and a Chair of Chemistry at Angarsk State Technical University.  
E-mail: [krivdin55@gmail.com](mailto:krivdin55@gmail.com)

## 1. Introduction

A breakthrough in the NMR studies of oil and oil refining products including light fractions, different types of fuels, heavy fractions, and crude oil itself provides a comprehensive structural elucidation of oil and oil refining products. The reviewed recent achievements and advances in this field are on the cutting edge of the modern oil refining chemistry and petrochemical industry.

Applications of experimental  $^1\text{H}$  and  $^{13}\text{C}$  NMR spectroscopy to the analysis of fuel in petroleum industry and oil refining technology are well covered in a number of reviews including that by Edwards.<sup>1</sup> Those studies are unfolding in parallel with significant progress in the computational NMR of hydrogen,<sup>2–4</sup> and carbon.<sup>5–10</sup> The present review discusses the recent advances in the NMR applications to the oil refining products, light fractions, various types of fuels, heavy fractions, and crude oil, as schematically shown in Fig. 1.

Generally, there is an overwhelming amount of publications dealing with application of NMR techniques to the structural elucidation of gasoline,<sup>11–17</sup> diesel,<sup>18–22</sup> kerosene,<sup>23–26</sup> distillate fractions,<sup>27,28</sup> and crude petroleum (see historical reference<sup>29</sup>) together with some other oil refining products. In the present brief review, we will by no means attempt to discuss in detail the application of NMR in this area. This review is only an overview of various NMR methods used for the structural elucidation of various oil refining products together with crude oil itself with particular emphasis on recent achievements and advances in this field.

$^1\text{H}$  and  $^{13}\text{C}$  NMR is also used in the fuel industry to estimate reservoir properties such as porosity, permeability, wettability, irreducible water saturation, and irreducible oil saturation.<sup>30</sup> In fact, the exploration and production of oil have essentially benefited from the application of NMR by effectively studying the evaluation of fuel properties.

Broadly speaking, typical  $^1\text{H}$  and  $^{13}\text{C}$  NMR chemical shift ranges of functional groups defining the composition of oil samples and their distillation products are given accordingly, in Tables 1 and 2.

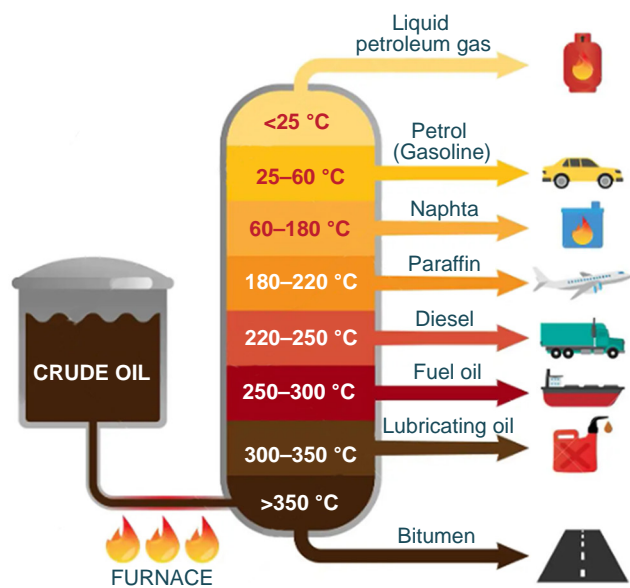


**Figure 1.** Basic types of fuel in the oil fractional distillation process. Reproduced with minor editing privilege from [https://www.123rf.com/photo\\_150445606\\_fractional-distillation-of-crude-oil-labeled-educational-explanation-scheme-diagram-with-chemical.html](https://www.123rf.com/photo_150445606_fractional-distillation-of-crude-oil-labeled-educational-explanation-scheme-diagram-with-chemical.html).

**Table 1.** Typical ranges of  $^1\text{H}$  NMR chemical shifts of functional groups defining the composition of oil samples. Compiled from Kalabin, Kanitskaya, and Kushnarev.<sup>31</sup>

Shift range, ppm	Functional group(s)
0.5–1.0	Mainly $\gamma$ - $\text{CH}_3$ -groups
1.0–1.7	Mainly $\beta$ - $\text{CH}_2$ -groups
1.9–2.1	$\alpha$ -Olefinic methyl groups
2.1–2.4	Methyl groups in $\alpha$ -position to aromatic carbons
2.4–3.5	$\text{CH}$ - and $\text{CH}_2$ -groups in $\alpha$ -position to aromatic carbons
3.5–4.5	Bridged $\text{CH}_2$ -groups between aromatic carbons
4.5–6.0	Olefinic protons
6.0–7.2	Monocyclic arenes
7.2–8.3	Aromatic protons
8.3–8.9	Deshielded aromatic protons
8.9–9.3	Tetracyclic arenes

## 2. NMR of fuel: recent advances and perspectives

### 2.1. Light fractions

Historically, Mühl and Srića<sup>13</sup> were the first to determine gasoline octane number by means of  $^1\text{H}$  NMR, which is exemplified with a spectrum presented in Fig. 2. In this paper, the correlation between octane number and the fluid catalytic cracking gasoline chemical composition was established according to the standard engine method and further tested by applying a linear regression analysis.

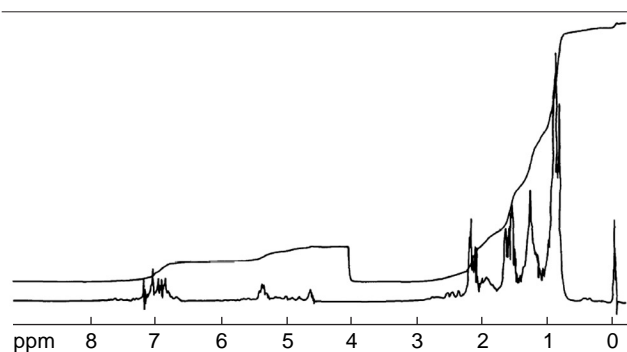
A decade or so later Meusenger<sup>12</sup> reported that  $^1\text{H}$  NMR allowed a rapid and accurate quantitative determination of the composition and quality of various gasolines. For this study, about 140 gasolines from Austrian filling stations were analyzed and the amounts of methanol, methyl *t*-butyl ether, and benzene together with other aromatic compounds were determined quantitatively using an internal standard.

**Table 2.** Typical ranges of  $^{13}\text{C}$  NMR chemical shifts of functional groups defining the composition of oil samples. Compiled from Kushnarev *et al.*<sup>32</sup>

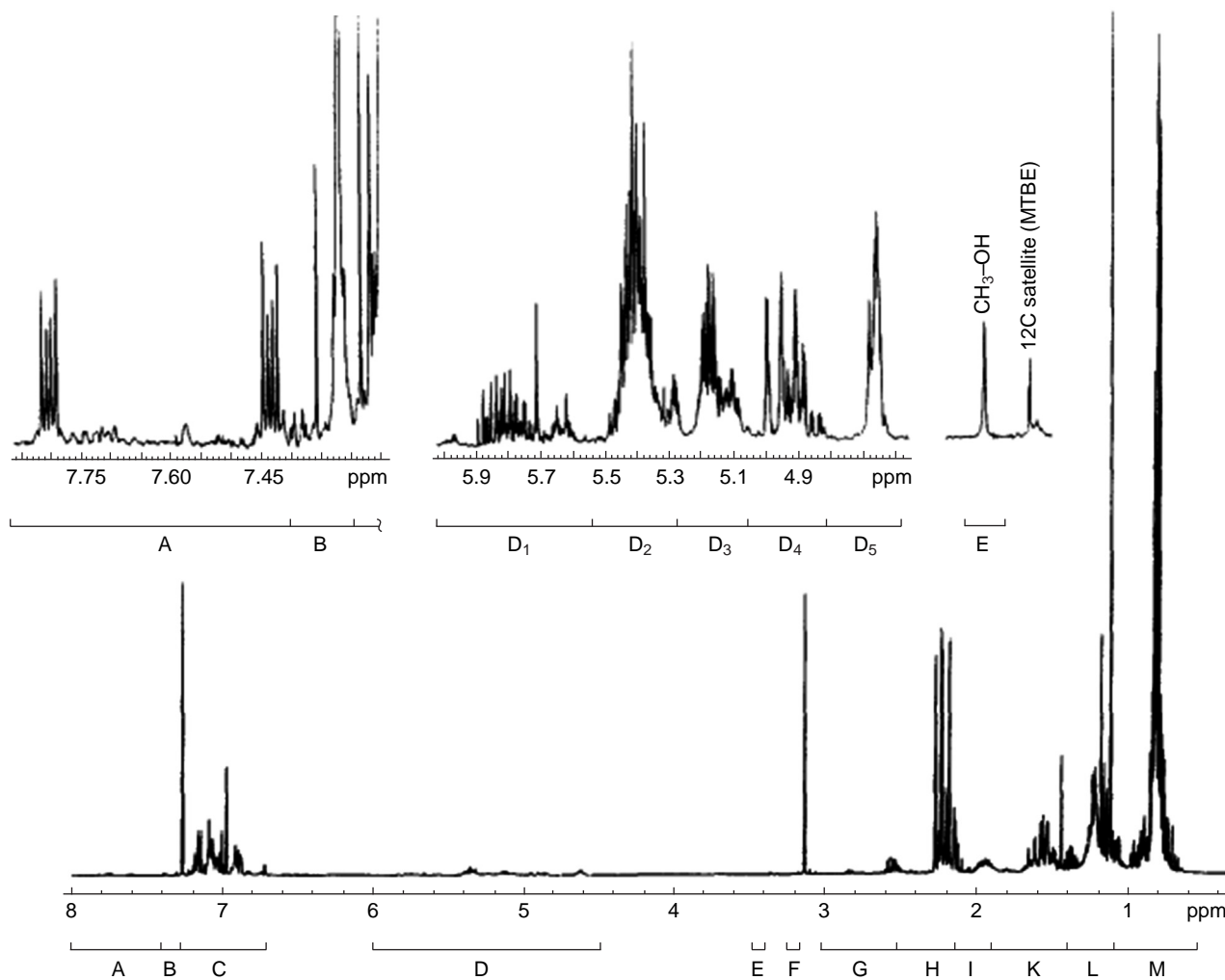
Shift range, ppm	Functional group(s)
11.0–12.5	$\gamma$ - $\text{CH}_3$ -groups, some aromatic $\text{CH}$ - and $\text{CH}_2$ -groups
12.5–15.0	$\gamma$ - $\text{CH}_3$ -groups in aromatic cycles
15.0–18.0	Olefinic $\beta$ - $\text{CH}_3$ -substituent
18.0–20.5	Shielded $\alpha$ - $\text{CH}_3$ -group, hydroaromatic and naphthenic $\alpha$ - $\text{CH}_3$ - and $\text{CH}_2$ -groups
20.5–22.5	Deshielded $\alpha$ - $\text{CH}_3$ -group, hydroaromatic and naphthenic $\alpha$ - $\text{CH}_3$ - and $\text{CH}_2$ -groups
22.5–24.0	$\gamma$ - $\text{CH}_2$ -groups; tetralinic $\beta$ - $\text{CH}_2$ -groups
24.0–27.5	Naphthenic $\text{CH}_2$ -groups; propyl and indane $\alpha$ - $\text{CH}$ - and $\beta$ - $\text{CH}_2$ -groups; isopropyl $\beta$ - $\text{CH}_3$ -group
27.5–37.0	Cyclic $\text{CH}_2$ -groups
37.0–60.0	Methine groups; naphthenic $\text{CH}$ and $\text{CH}_2$ alkyl groups, adjacent to $\text{CH}$ group
108.0–118.0	Olefinic carbons
118.0–129.5	Aromatic protonated carbons
129.5–133.0	Internal aromatic carbons
133.0–135.0	Methyl substituted arenes
135.0–138.0	Arenes, substituted naphthenes
138.0–160.0	Alkyl substituted arenes, N,O,S-heteroatomic arenes
165.0–175.0	Ester or amide carboxy carbon
170.0–182.0	Acid carboxy carbon
182.0–192.0	Quinone carboxy carbon
195.0–205.0	Aldehyde carbonyl carbon
202.0–220.0	Ketone carbonyl carbon

Figure 3 shows a typical  $^1\text{H}$  NMR spectrum of unleaded EuroSuper gasoline in  $\text{CDCl}_3$ . The chemical shift scale was divided by the author into 12 regions, marked A to M, as shown in this figure. The regions A, D, and E are magnified for clarity. The signals in the chemical shift region between 4.6 and 6 ppm, connected with the protons bonded to unsaturated carbons in olefins, were divided into five substructure groups (from  $\text{D}_1$  to  $\text{D}_5$ ). The small signal at 3.42 ppm (E, methyl protons of methanol) is in the range of the  $^{13}\text{C}$  satellites of the methyl *t*-butyl ether signal (3.37 ppm). A more detail specification of A to M ranges is given in Table 3.

Kapur, Singh, and Sarpal<sup>15</sup> developed a quantitative  $^1\text{H}$  NMR-based method for determining the composition of aromatics, naphthenes, and paraffins of straight-run gasoline fractions. In this paper the authors derived the equations



**Figure 2.** The 90 MHz  $^1\text{H}$  NMR spectrum of a neat fluid catalytic cracking gasoline. Reproduced from Mühl and Srića<sup>13</sup> with the permission of Elsevier.



**Figure 3.** The  $^1\text{H}$  NMR spectrum of a typical neat EuroSuper gasoline sample. The regions A to M are specified in the spectrum, and regions A, D and E are zoomed vertically by a factor of 80. Reproduced from Meusenger<sup>12</sup> with the permission of Elsevier.

**Table 3.**  $^1\text{H}$  NMR chemical shifts of structural fragments of gasolines. Compiled from Meusenger.<sup>12</sup>

Region	Chemical shift range, ppm	Structural group(s)	Integral region
1	8.0–7.4	Naphthalene	A
2	7.4–7.3	Benzene	B
3	7.3–6.7	Substituted aromatics	C
4	6.0–5.5	HHC=CHR	D <sub>1</sub>
	5.5–5.25	RCH=CHR	D <sub>2</sub>
	5.25–5.05	RRC=CHR	D <sub>3</sub>
	5.05–4.8	HHC=CHR	D <sub>4</sub>
	4.8–4.6	HHC=CRR	D <sub>5</sub>
5	3.5–3.3	CH <sub>3</sub> -OH	E
6	3.2–3.0	CH <sub>3</sub> -OC(CH <sub>3</sub> ) <sub>3</sub>	F
7	3.0–2.7	Ph-CH	G <sub>1</sub>
	2.7–2.5	Ph-CH <sub>2</sub>	G <sub>2</sub>
8	2.5–2.1	Ph-CH <sub>3</sub> and C=C-CH	H
9	2.1–1.85	C=C-CH <sub>2</sub>	I
10	1.85–1.4	CH, CH <sub>2</sub> (cycl.), C=C-CH <sub>3</sub>	K
11	1.4–1.1	CH <sub>2</sub> , C=C-C-CH <sub>2</sub> , Ph-C-CH <sub>3</sub>	L
12	1.1–0.5	CH <sub>3</sub>	M

necessary to calculate these compounds from the overlapped  $^1\text{H}$  NMR spectra with particular emphasis on signals from naphthenes and isoparaffins.

Figure 4 shows a typical  $^1\text{H}$  NMR spectrum of the straight-run petroleum cut. In this spectrum, region A is characteristic of aromatics, while signals due to the  $\alpha$ -substituents appear in regions B and C. The region between 0.5 and 2.05 ppm is highly

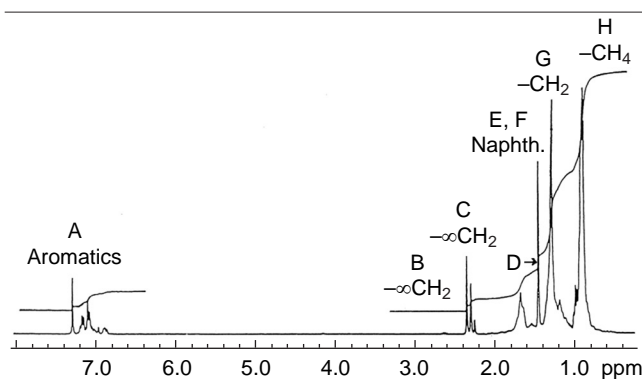


**Figure 4.** The 300 MHz  $^1\text{H}$  NMR spectrum of a representative straight-run gasoline fraction in  $\text{CDCl}_3$ . Reproduced from Kapur *et al.*<sup>15</sup> with the permission of Elsevier.

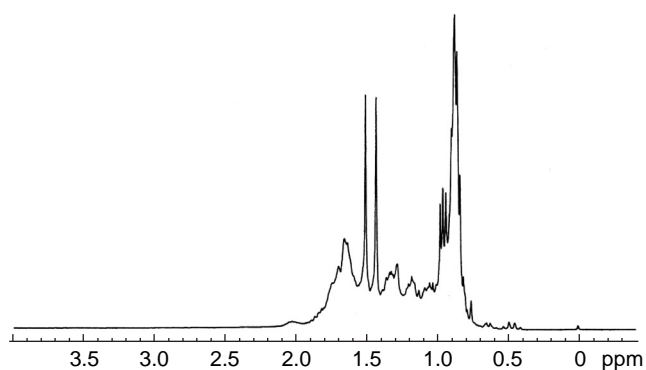


**Figure 5.** The 300 MHz  $^1\text{H}$  NMR spectrum of a standard naphthene mixture in  $\text{CDCl}_3$ . Reproduced from Kapur *et al.*<sup>15</sup> with the permission of Elsevier.

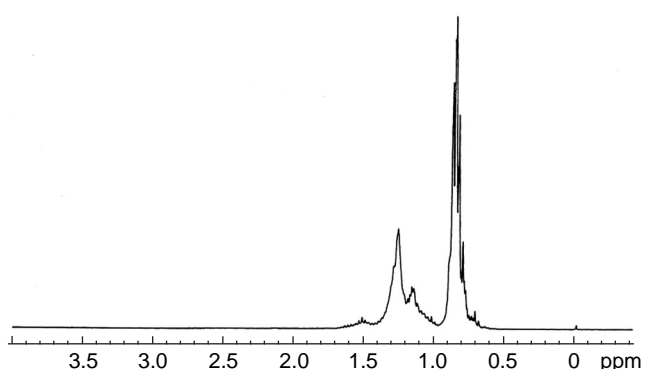


**Figure 6.** The 300 MHz  $^1\text{H}$  NMR spectrum of a standard isoparaffin mixture in  $\text{CDCl}_3$ . Reproduced from Kapur *et al.*<sup>15</sup> with the permission of Elsevier.

overlapped and contains signals mainly of cycloalkanes (naphthenes), normal and isoparaffins. The regions 0.5–1.0 ppm (H) and 1.0–1.4 ppm (G) are due to the  $\text{CH}_3$  and  $\text{CH}_2$  groups, respectively. Figures 5 and 6 show  $^1\text{H}$  NMR spectrum of the standard naphthene and isoparaffin mixtures consisting of different types of cycloalkane molecules with boiling points in the gasoline range.

In a later paper by the same principal authors,<sup>33</sup> the developing of a direct and fast method based on the  $^1\text{H}$  NMR spectroscopy for determining paraffins (P), olefins (O), naphthenes (N) and aromatics (A), abbreviated as ‘PONA’ was reported. Using this method, the composition of fluid catalytic cracking gasoline and coker gasoline containing olefinic hydrocarbons was established, as illustrated in Figs 7 and 8. The analysis performed showed that the PONA content of the fluid catalytic cracking gasoline and coker gasoline samples could be easily estimated using NMR spectral integral data without the use of standards. The method was announced to be convenient, accurate, and less time-consuming than gas chromatography and mass spectrometry used for the same purpose.

Jameel *et al.*<sup>16</sup> suggested an improved model for the prediction of ignition quality of hydrocarbon fuels by means of  $^1\text{H}$  NMR using a calibration set of cetane numbers of pure hydrocarbons and hydrocarbon blends of known composition by applying multiple linear regression modeling. In this study, a particular emphasis was placed on the effect of branching, and a new parameter denoted as the ‘Branching Index’ was introduced to quantify this effect in the series of 71 pure hydrocarbons and

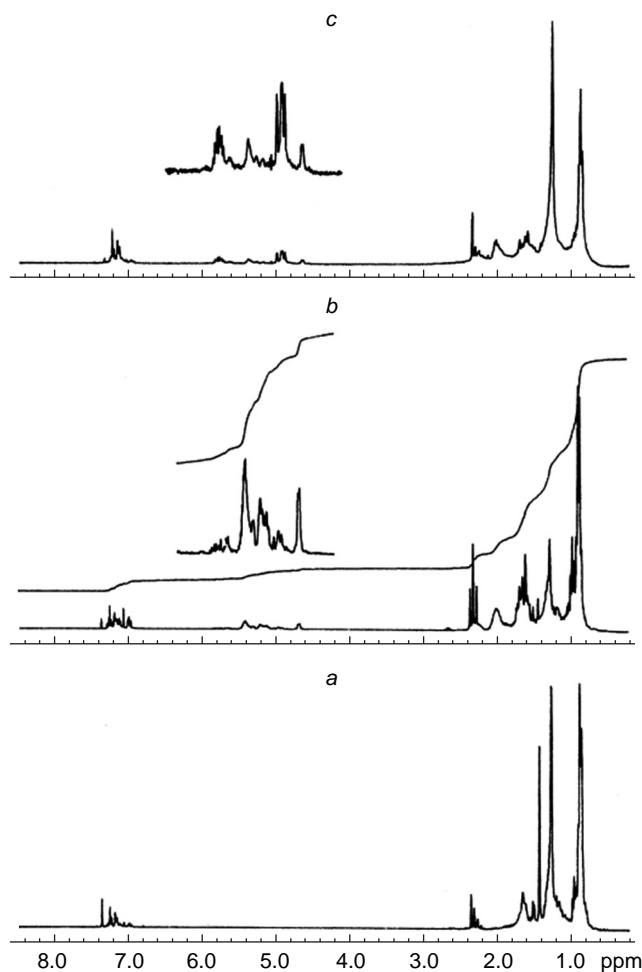


**Figure 7.** The 300 MHz  $^1\text{H}$  NMR spectra in  $\text{CDCl}_3$  of (a) straight-run naphtha; (b) fluid catalytic cracking gasoline; (c) coker gasoline. Reproduced from Sarpal *et al.*<sup>33</sup> with the permission of Elsevier.

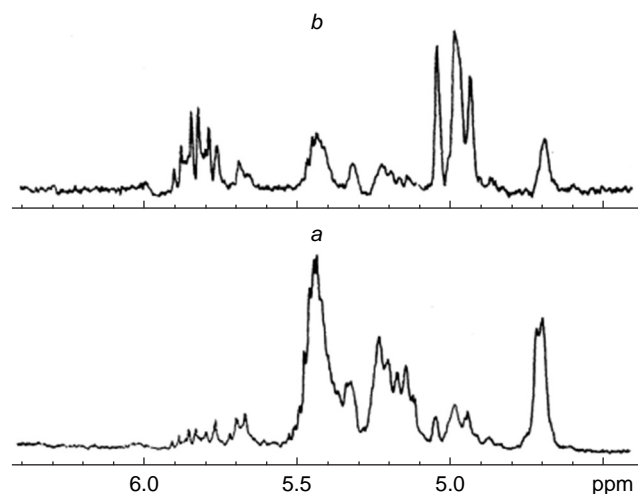


**Figure 8.** Olefinic region of 300 MHz  $^1\text{H}$  NMR spectra in  $\text{CDCl}_3$  of (a) fluid catalytic cracking gasoline; (b) coker gasoline. Reproduced from Sarpal *et al.*<sup>33</sup> with the permission of Elsevier.

54 hydrocarbon blends. The developed model was validated with experimentally measured cetane numbers of 22 real gasolines and 59 blends of known composition, and predicted values were found to match well with experimental data.

Later the same lead authors<sup>17</sup> presented a novel approach to surrogate fuel by minimizing the number of surrogate species. Five key functional groups, namely paraffinic CH<sub>3</sub>, CH<sub>2</sub>, and CH, naphthenic CH–CH<sub>2</sub>, and aromatic C–CH groups, as well as structural information provided by the Branching Index, were chosen as matching targets. At that, six models of FACE (Fuels for Advanced Combustion Engines) gasoline target fuels were established. As a result of that study, five abovementioned functional groups of those fuels were qualitatively and quantitatively identified using high-resolution <sup>1</sup>H NMR spectroscopy, as illustrated by the <sup>1</sup>H NMR spectra of the model FACE gasoline fuels shown in Fig. 9, where the Branching Index for each surrogate molecule is provided in parenthesis.

In a very recent study Mondal and coauthors<sup>34</sup> proposed a powerful method for the accurate determination of various kinds of quaternary, methine, methylene, and methyl carbons in the light coker naphthas by means of the two-dimensional phase-sensitive gradient-selected edited Heteronuclear Single Quantum Coherence (known as ‘edited HSQC’), as illustrated in Fig. 10. The typical ranges of the <sup>1</sup>H NMR chemical shifts of the functional groups defining the composition of light coker naphthas are given in Table 4.

Comparison of these results with two standard chromatography-based methods for PONA estimation showed that the proposed method gave excellent correlations for the estimation of olefins and aromatics and, but relatively poor correlation for naphthenes. However, the authors stated, that this NMR method for PONA estimation is ‘rapid, free from manual error, highly repeatable, and best suitable for monitoring pilot plant reactions with high sample throughput’.<sup>34</sup>

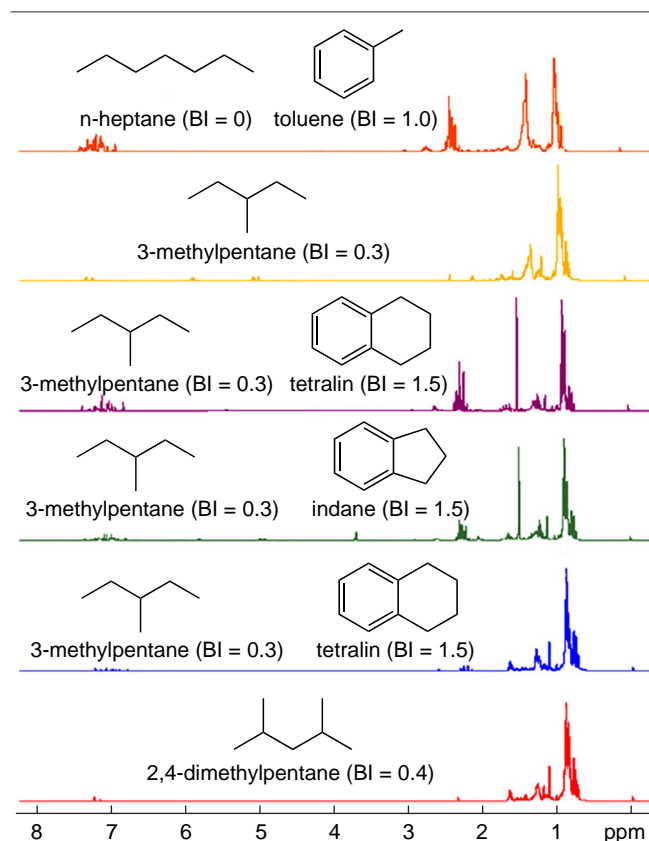


**Figure 9.** 700 MHz <sup>1</sup>H NMR spectra of the model FACE gasoline fuels in CDCl<sub>3</sub>. Reproduced with minor editing privilege from Jameel *et al.*<sup>17</sup> with the permission of Elsevier.

**Table 4.** Typical ranges of <sup>1</sup>H NMR chemical shifts of the functional groups defining the composition of light coker naphthas. Compiled from Mondal *et al.*<sup>34</sup>

Molecular fragment	Region, ppm
Bu <sup>t</sup> groups	0.92–1.10
Terminal CH <sub>3</sub>	0.40–1.22
Paraffinic CH <sub>2</sub>	1.22–1.40
Naphthenic CH <sub>2</sub>	1.40–1.58
Allylic CH <sub>3</sub>	1.58–1.75
Allylic CH <sub>2</sub>	1.75–2.08
Allylic CH (highfield)	2.08–2.28
α-CH <sub>3</sub> to aromatic rings	2.28–2.36
Allylic CH (lowfield)	2.36–3.00
Olefinic CH or CH <sub>2</sub>	4.40–6.50
Aromatic CH	7.44–8.00

Another example is the identification of conjugated diolefins made possible by the two-dimensional NMR experiments where the olefin resonances could not reveal the presence of protons adjacent to each other on conjugated olefin double bonds.<sup>1</sup> An example of the <sup>1</sup>H–<sup>1</sup>H COSY (CORrelated SpectroscopY) result obtained on a coker naphtha is shown in Fig. 11, taken from this publication. It can be seen that correlation of olefinic protons with adjacent olefinic and aromatic protons provides a distribution of conjugated diolefins which can then be quantified in the 1-dimensional NMR spectrum.

It is well known that the low magnetic fields permanent magnets are characterized by the high basic field homogeneity and tight magnet temperature control. Mechanical and electrical shim systems provide the high resolution NMR data at low magnetic fields. A typical <sup>1</sup>H NMR spectrum of a gasoline product obtained on such spectrometers is shown in Fig. 12.<sup>1</sup>

Light naphtha is a mixture consisting mainly of straight-chained and cyclic aliphatic hydrocarbons having from five to six carbon atoms per molecule, while heavy naphtha possess from seven to nine carbon atoms per molecule. Low boiling light naphtha is generally a hydrocarbon product that is somewhat interchangeable with natural gasoline and lease condensates. Although low boiling naphtha has properties similar to lease condensate and natural gasoline, it is considered to be a refined product since it is produced by refinery distillation or the process of condensate splitting. In fact, most naphthas are produced from crude oil in the first step of the refining process, distillation. Light naphtha is composed predominantly of pentane and hexane derivatives as well as smaller amounts of higher molecular weight hydrocarbons.

The <sup>1</sup>H NMR spectroscopy has been widely used for the structural elucidation of naphthas. Much structural information is provided by the <sup>1</sup>H NMR spectra of naphthas recorded at the frequencies of 400 MHz and higher. Below are a few examples of the <sup>1</sup>H NMR spectra of different naphthas (Light Naphthas, Straight-Run Naphthas, and Coker Naphthas) recorded at 400 MHz presented accordingly, in Figs 13–15.

## 2.2. Fuels

To compare the higher resolution of <sup>1</sup>H NMR experiments performed on superconducting NMR systems with those carried out on 60 MHz spectrometers, characteristic spectra of a diesel fuel recorded at 60 and 300 MHz are presented in Fig. 16. Although more peaks are resolved at 300 MHz, the overall chemical information obtained from these two NMR spectra

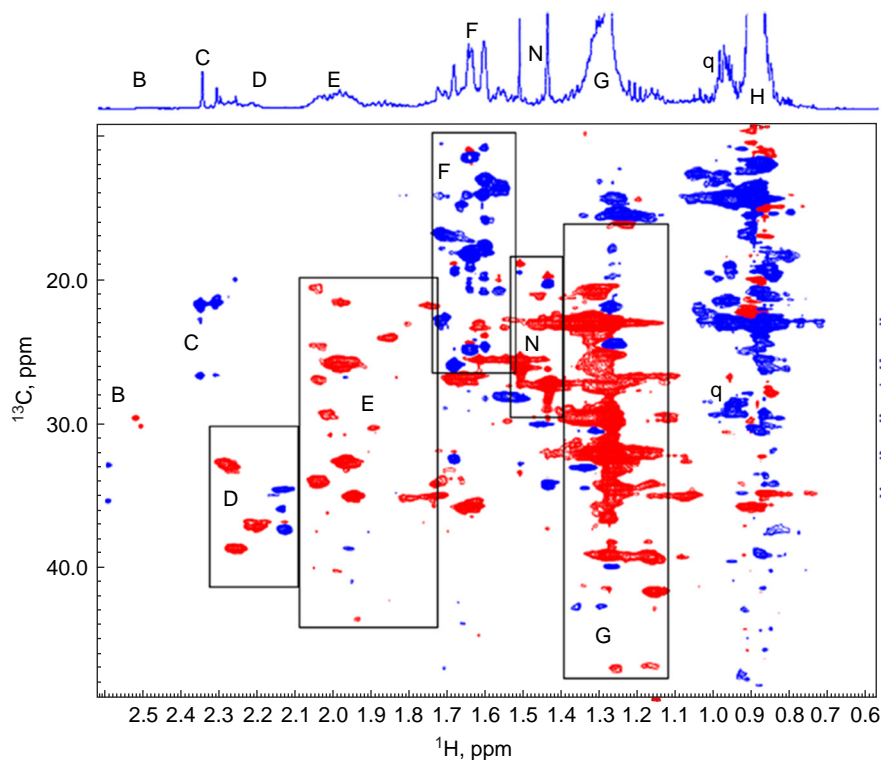


**Figure 10.** Edited HSQC spectrum ( $\text{CH}_2$  groups are in red;  $\text{CH}$  and  $\text{CH}_3$  groups are in blue) of a representative light coker naphtha sample in  $\text{CDCl}_3$ . Designation of regions are provided in Table 4. Reproduced from Mondal *et al.*<sup>34</sup> with the permission of the American Chemical Society.

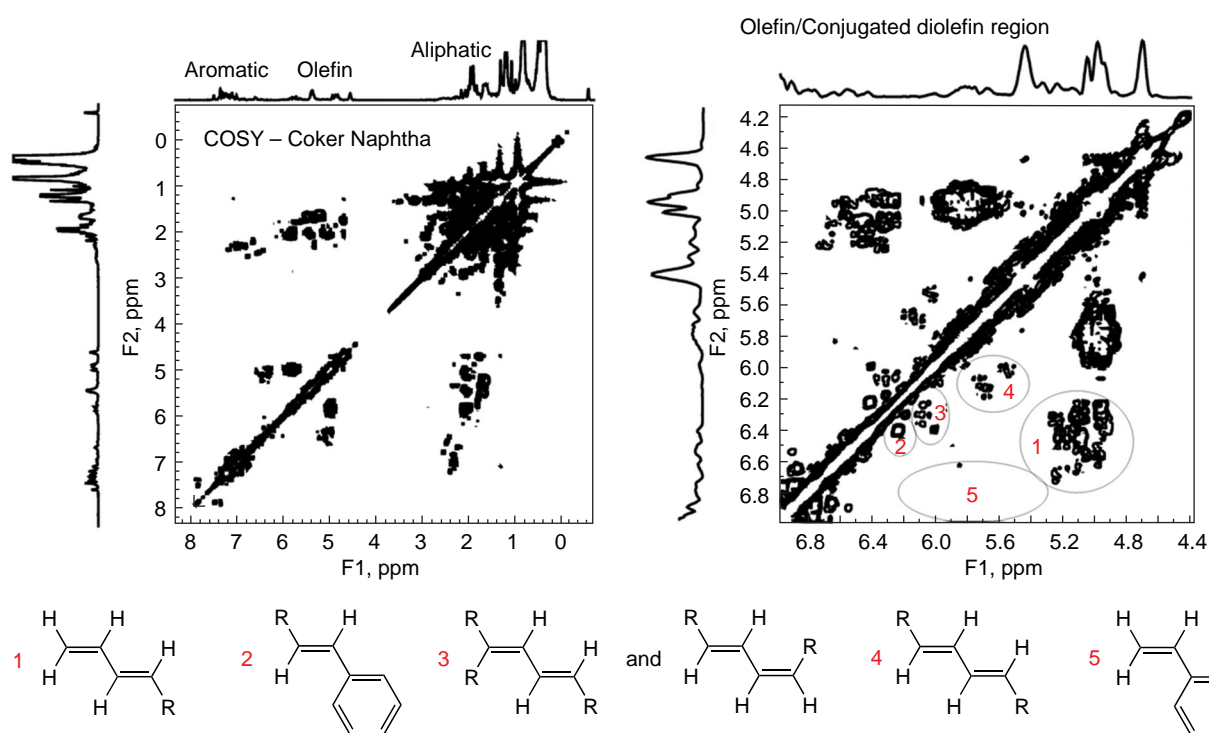


**Figure 11.**  $^1\text{H}$ – $^1\text{H}$  COSY of a coker naphtha stream in  $\text{CDCl}_3$ . Reproduced with minor editing privilege from Edwards<sup>1</sup> with the permission of ASTM International.

seems to be the same. In most cases NMR spectrometers with field strengths of 7–11.7 Tesla (corresponding to the  $^1\text{H}$  resonance frequencies of 300–500 MHz) are adequate for the liquid-phase petroleum applications, as the higher resolution at higher magnetic fields does not provide any extra chemical information.

Some examples of  $^{13}\text{C}$  NMR spectra of diesel fuels taken from Edwards<sup>1</sup> are shown in Fig. 17. In these spectra, cracked

diesel shows the presence of olefinic carbon, straight-run diesel shows a narrow distribution of aromatics, while naphthenic diesel displays a typical ‘hump’ in the aliphatic carbon region, which can be attributed to the fraction of naphthenic and paraffinic carbons.

It is well known that the Distortionless Enhancement by Polarization Transfer (DEPT) technique allows the separate observation of methyl ( $\text{CH}_3$ ), methylene ( $\text{CH}_2$ ), methane ( $\text{CH}$ ),

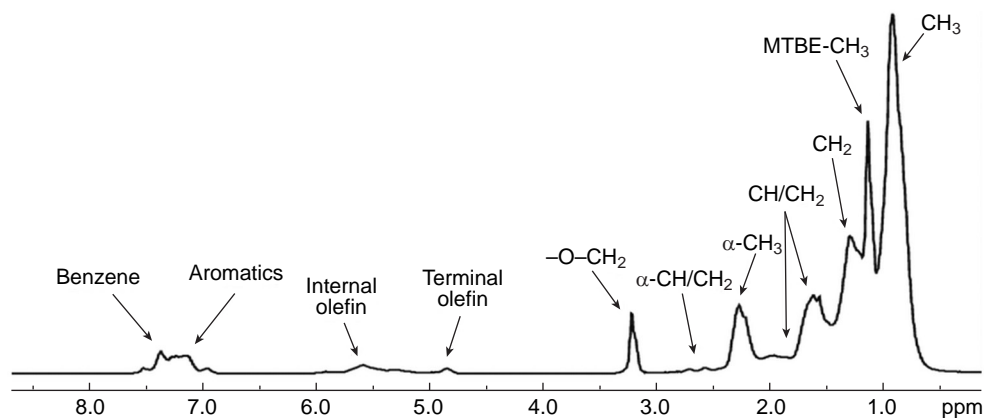


**Figure 12.** The 60 MHz  $^1\text{H}$  NMR spectrum of a neat gasoline obtained on a process NMR unit. Reproduced with minor editing privilege from Edwards<sup>1</sup> with the permission of ASTM International.

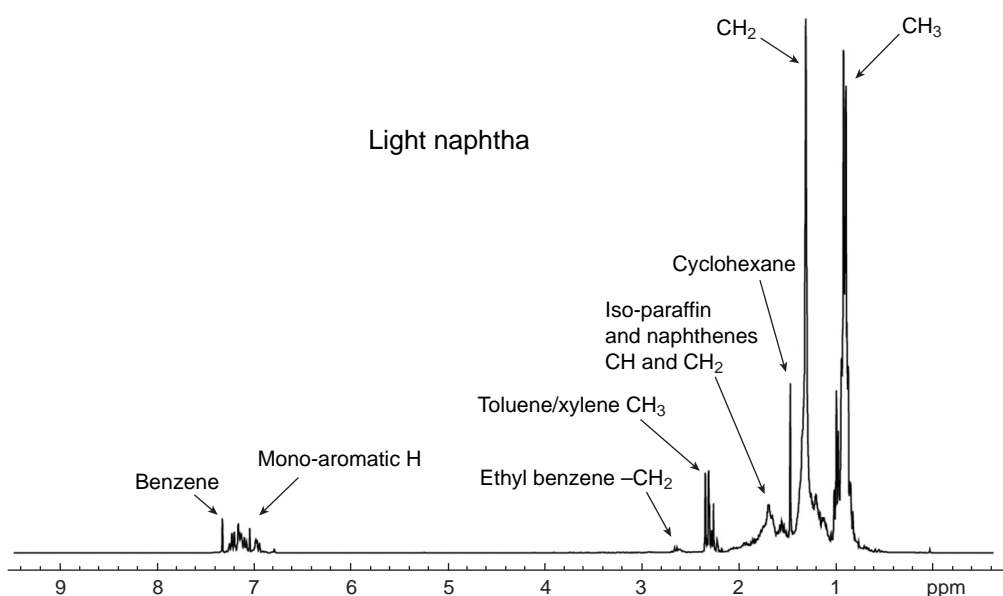


**Figure 13.** The typical 400 MHz  $^1\text{H}$  NMR spectrum of neat light naphtha. Reproduced with minor editing privilege from <https://process-nmr.com/naphtha-analysis-by-nmr/> (Process NMR Associates) under the CC BY-NC 4.0 International Public License.

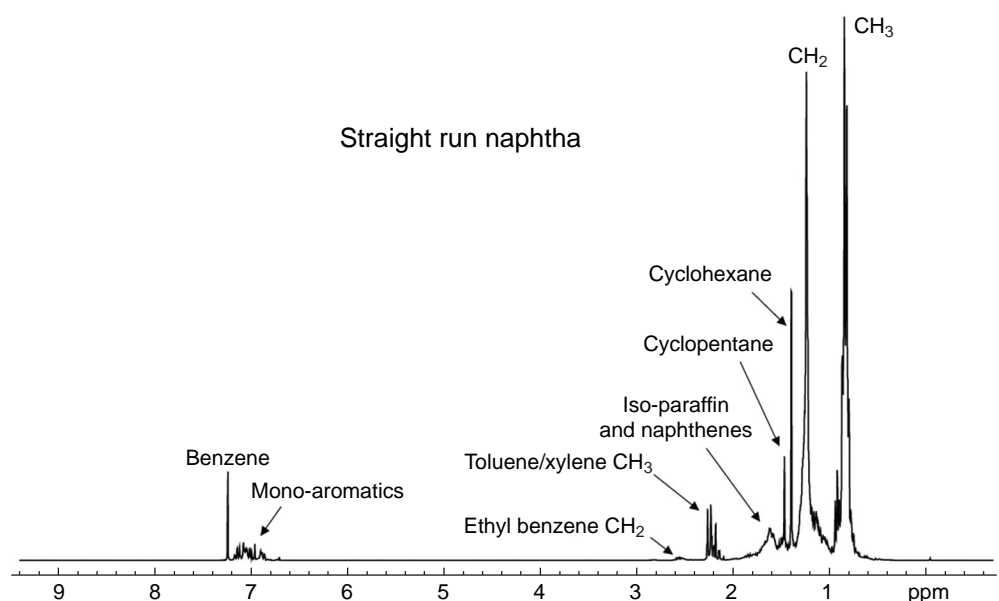


**Figure 14.** The typical 400 MHz  $^1\text{H}$  NMR spectrum of neat straight-run naphtha. Reproduced with minor editing privilege from <https://process-nmr.com/naphtha-analysis-by-nmr/> (Process NMR Associates) under the CC BY-NC 4.0 International Public License.

and quaternary carbons of a petroleum product. For the oil refining products, this technique provides the analysis of hydrocarbon branching and calculation of aromatic ring system sizes. An example of a DEPT NMR spectrum of diesel fuel is

shown in Fig. 18 taken from Edwards.<sup>1</sup> Further comparison of DEPT results with the quantitative  $^{13}\text{C}$  NMR single pulse excitation spectrum allows to identify and quantify the quaternary carbons. It also allows further calculation of the

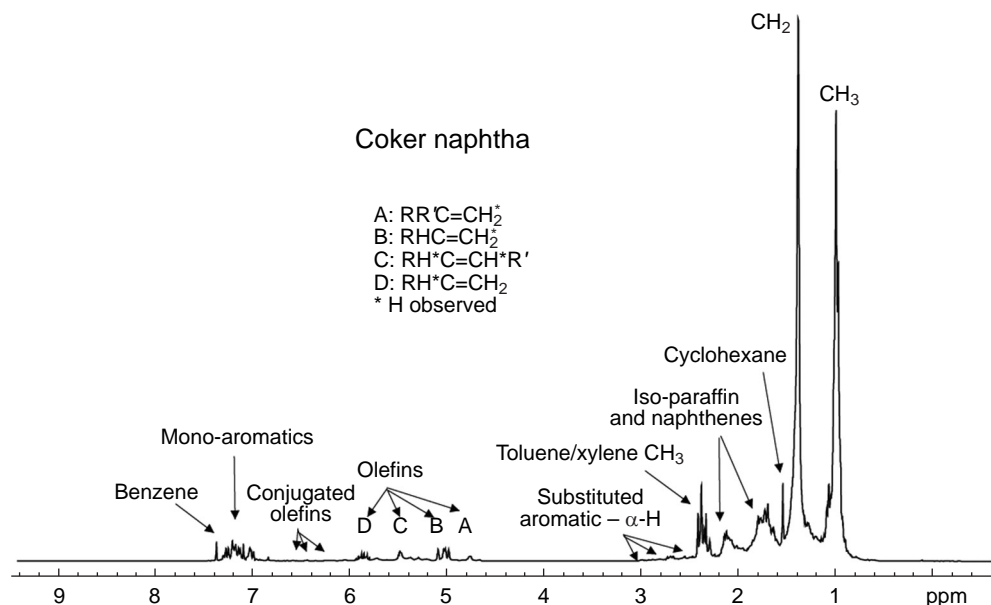


**Figure 15.** The typical 400 MHz  $^1\text{H}$  NMR spectrum of neat coker naphtha. Reproduced with minor editing privilege from <https://process-nmr.com/naphtha-analysis-by-nmr/> (Process NMR Associates) under the CC BY-NC 4.0 International Public License.

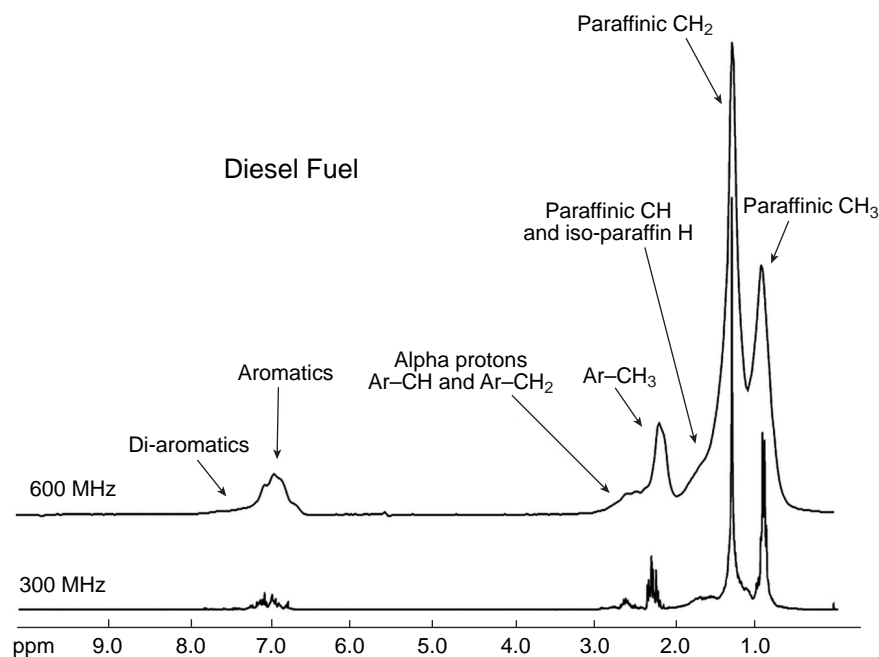


**Figure 16.**  $^1\text{H}$  NMR spectrum of neat diesel fuel at different resonance frequencies. Reproduced with minor editing privilege from Edwards<sup>1</sup> with the permission of ASTM International.

average aromatic ring size and other average molecule parameters describing the petroleum product, so that the entire refinery process can be analyzed and monitored.

Important information can be obtained from the  $^{13}\text{C}$  NMR of diesel fuels, such as average chain length, alkyl substitution, aromatic carbon distribution, *iso*-paraffin content, and branching index. It is well known that (1) higher branching leads to lower oxidation stability; (2) increase in average alkyl chain length leads to increase in viscosity; (3) branching index and naphthenic content increase while normal paraffin content and aromatic content decrease; (4) decrease in aromatic carbon and increase in saturated carbon leads to increase in viscosity index during hydrogenation; (5) average chain length of paraffinic base oils decreases with hydrogenation.<sup>35</sup>

$^{13}\text{C}$  NMR is uniquely suited to analyze branching structures of *iso*-paraffins. Approaches to their analysis include the use of DEPT experiments to identify either CH carbons at branching points or  $\text{CH}_3$  carbons whose chemical shift varies depending on

the proximity of a molecule end or a branch point.<sup>1</sup> As an example, Fig. 19 shows the peaks in the aliphatic region of the  $^{13}\text{C}$  NMR spectrum.

Ure, O'Brayen, and Dooley<sup>36</sup> suggested a detailed experimental methodology for the measurement of quantitative  $^1\text{H}$  and  $^{13}\text{C}$  NMR spectra of liquid hydrocarbons. They determined optimal experimental conditions (pulse width, time delay, relaxant, solvent), which allowed the registration of the 'entirely quantitative'  $^1\text{H}$  and  $^{13}\text{C}$  NMR spectra of liquid hydrocarbons illustrated in Fig. 20. The uncertainty associated with these measurements was generally found to be less than 3%; but this did not take into account overlapping peaks.

In general, the use of the HSQC method allows the determination of the fuel-specific integral regions, and, most importantly, was shown to be a convenient method for the identification of overlapping peaks in the two-dimensional spectra, see Figs 21 and 22. In particular, Region 1 in Fig. 21 shows the overlap between the CH of *iso*-octane with three of

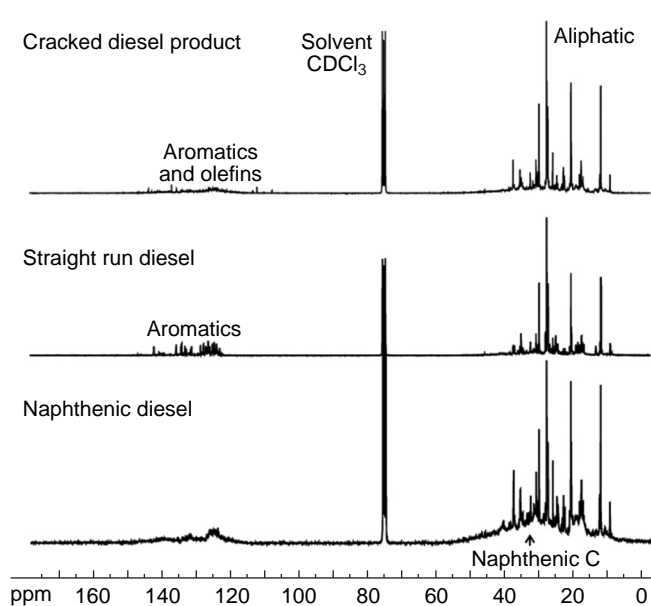


**Figure 17.** Quantitative  $^{13}\text{C}$  NMR spectra of three neat diesel fuels from different refinery processes. Reproduced with minor editing privilege from Edwards<sup>1</sup> with the permission of ASTM International.

the  $\text{CH}_2$  atom types in methylcyclohexane. Region 2 shows the overlap of the CH in methylcyclohexane, two of the  $\text{CH}_2$  atom types in methylcyclohexane, and all the  $\text{CH}_2$  atom types in *n*-decane. Region 3 shows overlap of a  $\text{CH}_2$  atom type from methylcyclohexane, the  $\text{CH}_3$  atom type from methylcyclohexane, and the  $\text{CH}_3$  atom type from *n*-decane. In general, the main purpose of this publication<sup>36</sup> was to experimentally determine and demonstrate the effective experimental conditions required to obtain quantitative  $^1\text{H}$  and  $^{13}\text{C}$  NMR results in typical liquid transportation fuels.

Jameel and coauthors<sup>11</sup> proposed using NMR spectroscopy in combination with Artificial Neural Networks (ANN) to predict the octane numbers of a range of FACE, namely the Research Octane Numbers (RON) and the Motor Octane Numbers (MON). The RON and MON are the two most

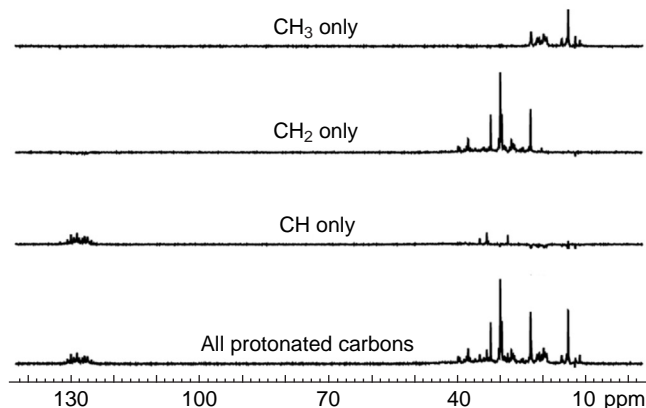


**Figure 18.**  $^1\text{H}$ - $^{13}\text{C}$  DEPT NMR of a neat diesel fuel showing the calculated subspectra for  $\text{CH}_3$ ,  $\text{CH}_2$ , and CH carbons. Quaternary carbons are not observed in this experiment. Reproduced from Edwards<sup>1</sup> with the permission of ASTM International.

commonly employed octane ratings for fuels used worldwide. In particular, RON is measured by running the fuel in a cooperative fuel research engine under standard test conditions followed by NMR monitoring.

In this paper, the effect of a number of functional groups including methyl, methylene, methyne, olefinic, naphthenic, and aromatic groups on the octane number of fuels was studied and some useful correlations were suggested. In particular, good correlations ( $R^2 \approx 0.99$ ) were found between experimental and predicted values of RON and MON based on the comparison of 57 points randomly selected to validate this model for pure hydrocarbons together with hydrocarbon-ethanol and FACE gasoline-ethanol mixtures (see Fig. 23).

### 2.3. Asphaltenes

In the crude oil production and processing, asphaltene aggregation and subsequent precipitation is a major problem for the oil industry leading to deactivation of catalysts, blocking pipelines, and deposition on the internal surface of the vessels. Asphaltenes, a complex natural mixture of compounds, consist

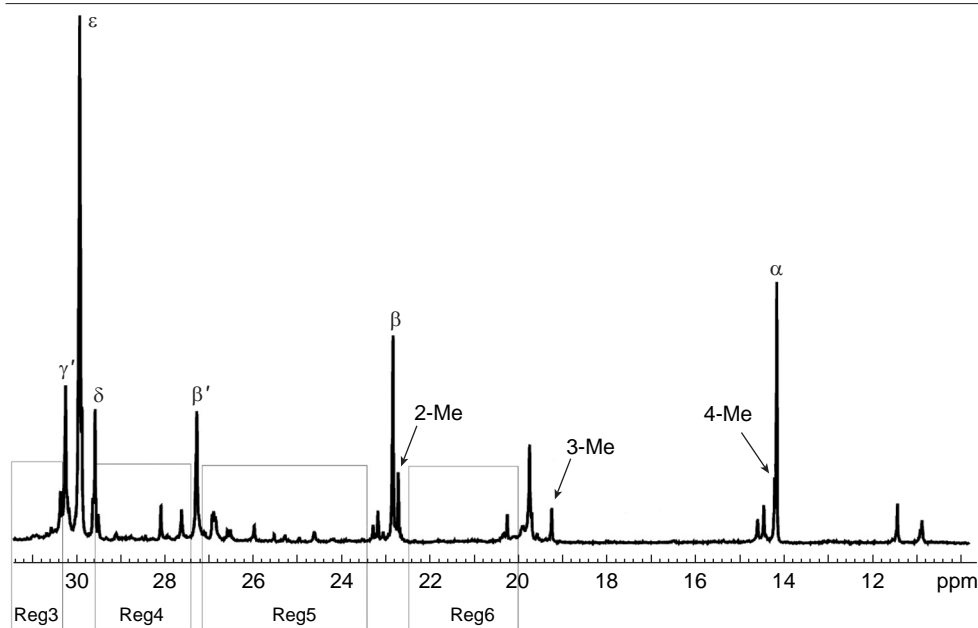


**Figure 19.** Identification of peaks associated with various pendant and terminal methyl carbons in the aliphatic carbon region of the neat  $^{13}\text{C}$  NMR spectrum. Also identified are the  $\alpha$ ,  $\beta$ ,  $\gamma$ ,  $\delta$ , and  $\epsilon$  resonances due to carbons in linear regions of a paraffin chain and the  $\beta'$  and  $\gamma'$  resonances which are methylenes two and three carbons away from a branch point. For used abbreviations, see original text. Reproduced from Edwards<sup>1</sup> with the permission of ASTM International.

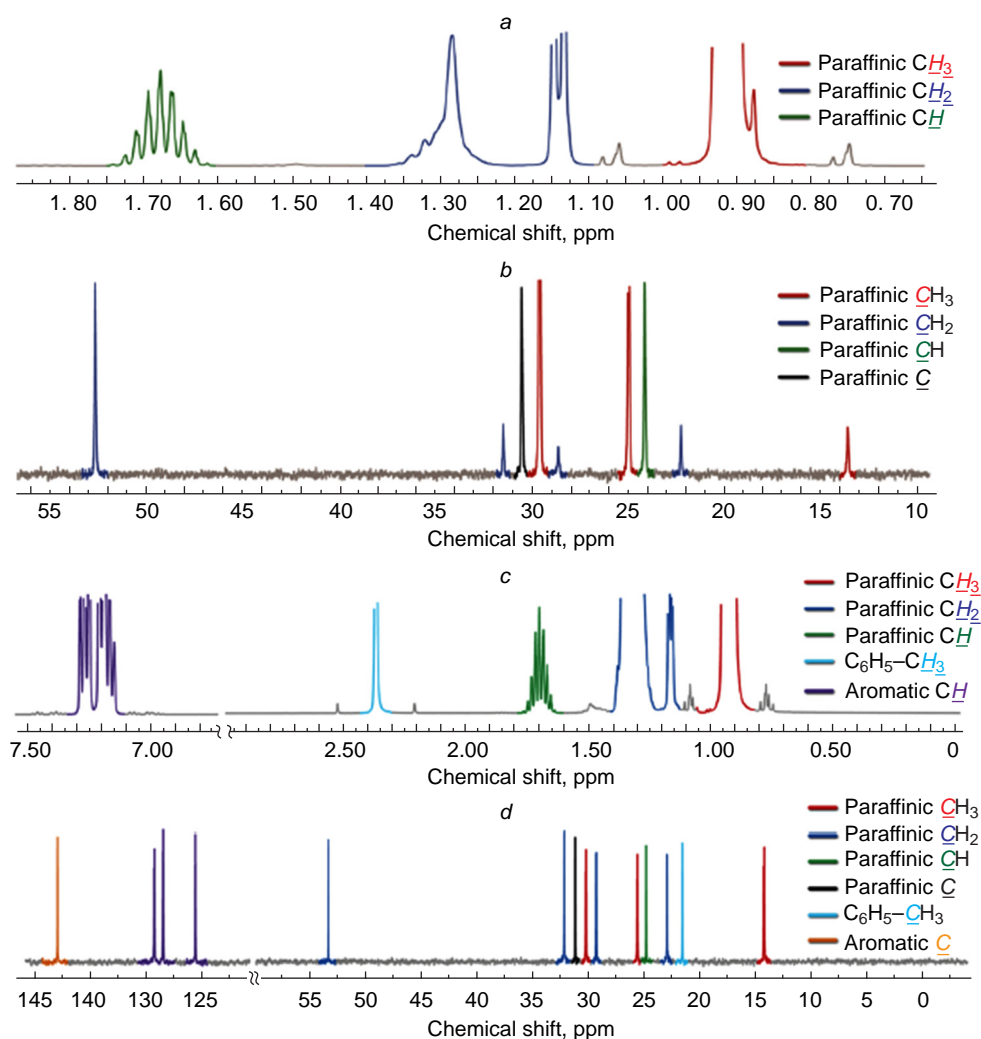


**Figure 20.** (a)  $^1\text{H}$  NMR spectrum of the Primary Reference Fuel «89», PRF89 (0.05 g) in  $\text{CD}_2\text{Cl}_2$  (1.0 g) at 400 MHz; (b)  $^{13}\text{C}$  NMR spectrum of PRF89 (0.2 g) with 0.05 M  $\text{Cr}(\text{acac})_3$  in  $\text{CDCl}_3$  (0.8 g) at 101 MHz; (c)  $^1\text{H}$  NMR spectrum of the Toluene Reference Fuel, TRF (0.05 g) in  $\text{CD}_2\text{Cl}_2$  (1.0 g) at 400 MHz; (d)  $^{13}\text{C}$  NMR spectrum of the TRF (0.2 g) with 0.05 M  $\text{Cr}(\text{acac})_3$  in  $\text{CDCl}_3$  (0.8 g) at 101 MHz. Reproduced with minor editing privilege from Ure *et al.*<sup>36</sup> with the permission of the American Chemical society.

of aromatic cores bonded to aliphatic and aromatic molecules containing heavy metals. NMR spectroscopy is largely used to characterize the chemical structure of asphaltenes and their chemical behavior, as recently reviewed by Ok and Mal.<sup>37</sup>

Among many other related studies, Andrews and coworkers<sup>38</sup> performed a comparison of coal-derived and petroleum asphaltenes using  $^{13}\text{C}$  NMR, demonstrating that the molecular sizes of the coal-derived asphaltenes were substantially smaller than those of the original petroleum asphaltenes. It was found that interior bridgehead carbons were an important component of asphaltenes and that correct consideration of these carbons allowed the number of fused rings in the sample to be correctly determined. It was also established that the petroleum asphaltenes contained significantly more carbons in chains of at least 9 carbons in length than the coal-derived asphaltenes.

The average chain lengths derived by this method were relatively short, but this did not mean that the aliphatic chain lengths in petroleum asphaltenes were about 3–4 carbons long, as previously thought. The peaks labeled  $\alpha$ ,  $\beta$ ,  $\gamma$ ,  $\delta$ , and  $\epsilon$  in Figure 24 aroused from terminal carbons ( $\alpha$ , 14 ppm) and carbons that were one ( $\beta$ , 22.7 ppm), two ( $\gamma$ , 32 ppm), three ( $\delta$ , 29.7 ppm), four ( $\epsilon$ , 30.1 ppm) or even more carbons away from the terminal carbon. Integration of those peaks yielded the number of carbons in the linear paraffins. In coals, these paraffins were found to be present at low levels (below 3%) and were relatively shorter and present in a wider range of chemical configurations than the petroleum asphaltenes. Naphthenic carbons and *iso*-

paraffins accounted for the remaining saturated carbon intensity. On the contrary, petroleum asphaltenes were shown to have roughly 50% aromatic carbons, whereas in the coal-derived asphaltenes the contents of aromatic carbons was close to 80%, as can be easily established by  $^{13}\text{C}$  NMR (see Fig. 25).

Only protonated carbons were observed in the DEPT spectra of asphaltenes. To calculate the relative amount of paraffinic  $\text{CH}_3$  to aromatic  $\text{CH}$  and obtain a quantitative ratio, a simple ratio calculation was performed. This ratio was then applied to the quantitative  $^{13}\text{C}$  NMR data to subtract out the protonated aromatic carbons. Comparison with the signal intensities observed in the quantitative spin-echo experiments, allowed to the authors<sup>38</sup> to determine the amount of nonprotonated carbons presented in the aromatic region of the spectrum, as illustrated in Fig. 26.

Later Fergoug and Bouhadda<sup>39</sup> examined structural parameters of asphaltenes derived from the Algerian Hassi Messaoud oil field by means of both  $^1\text{H}$  and  $^{13}\text{C}$  NMR. The main finding of this study was that the asphaltenes studied contained approximately seven condensed aromatic rings attached to short aliphatic chains of 4 to 6 carbons. The  $^1\text{H}$  and  $^{13}\text{C}$  NMR spectra of a sample asphaltene from this series are presented in Figs 27 and 28, the latter showing  $^{13}\text{C}$  NMR spectra for aliphatic (a) and aromatic (b) carbons separately.

Typical ranges of  $^1\text{H}$  and  $^{13}\text{C}$  NMR chemical shifts of various asphaltenes are given accordingly in Tables 5 and 6 compiled from Ok and Mal.<sup>37</sup>

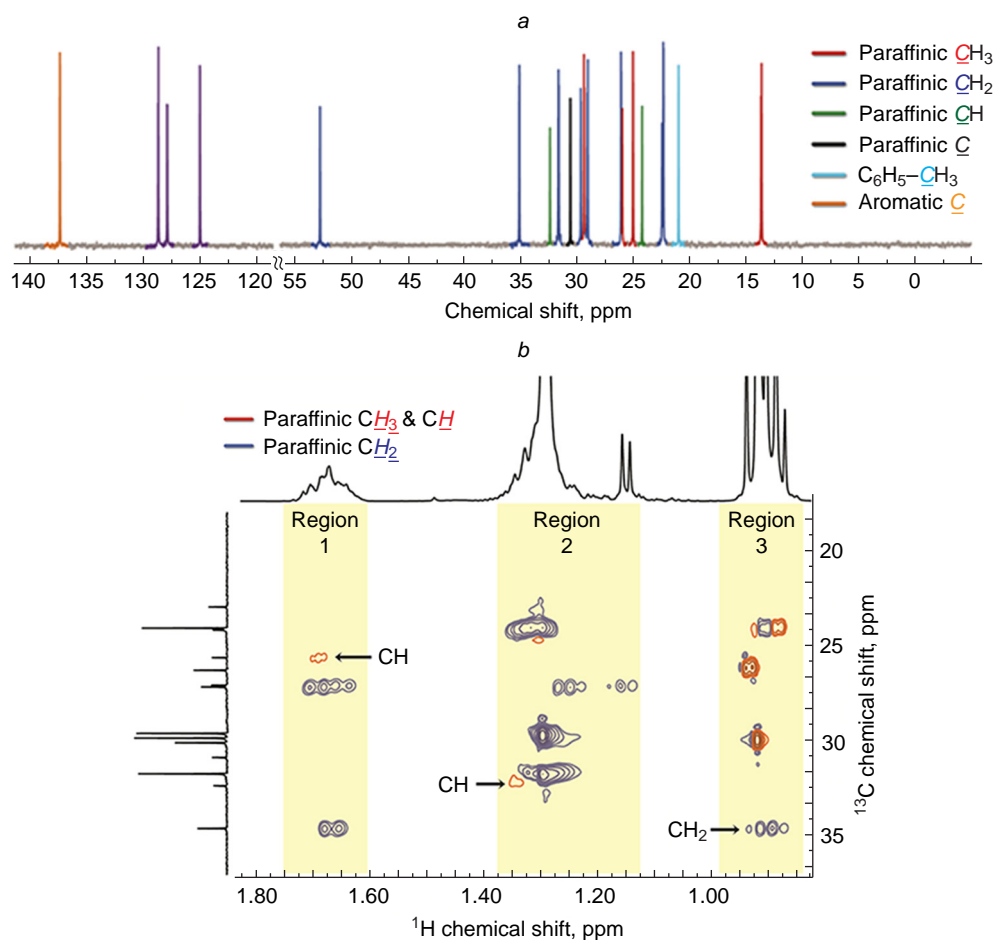


**Figure 21.** (a)  $^{13}\text{C}$  NMR spectrum of model fuel (0.2 g) with 0.05 M  $\text{Cr}(\text{acac})_3$  in  $\text{CDCl}_3$  (0.8 g) at 101 MHz; (b) phase-edited HSQC spectrum of Model Fuel (0.05 g) in  $\text{CD}_2\text{Cl}_2$  (1.0 g) at 600 MHz. Reproduced with minor editing privilege from Ure *et al.*<sup>36</sup> with the permission of the American Chemical Society.

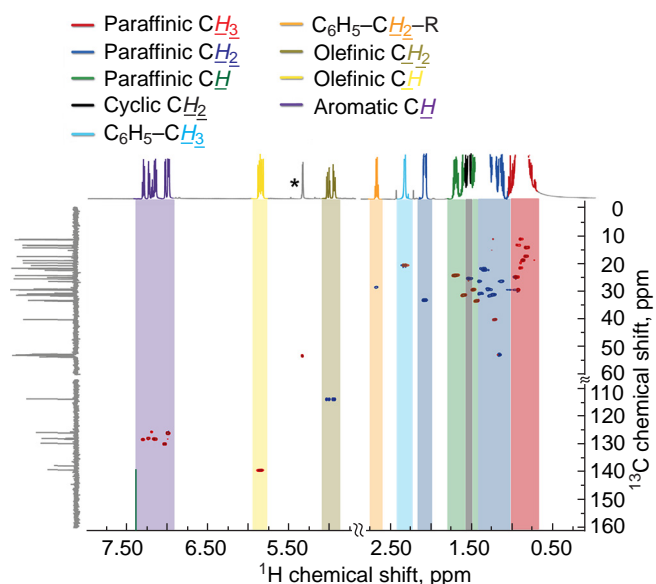


**Figure 22.** Phase-edited HSQC spectrum of model fuel (0.05 g) in  $\text{CD}_2\text{Cl}_2$  (1.0 g) at 600 MHz. Reproduced from Ure *et al.*<sup>36</sup> with the permission of the American Chemical Society.

## 2.4. Crude oil

NMR has unique advantages in the geochemical analysis of crude oil because it can provide robust information on chemical functional groups including those in aliphatic hydrocarbons,

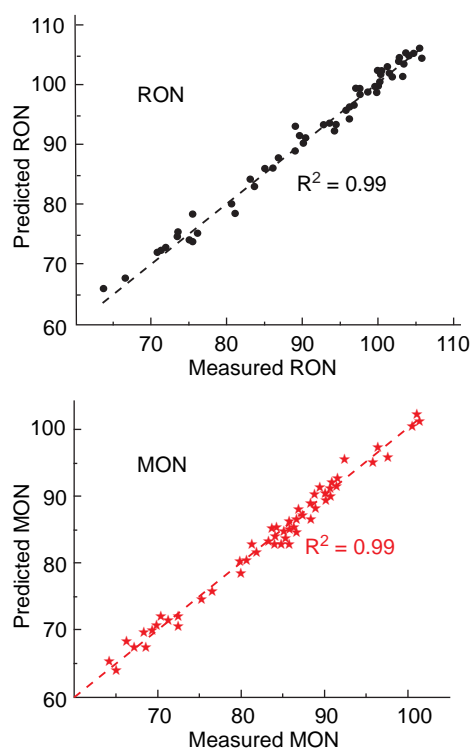


**Figure 23.** Correlation plots of measured vs. predicted RON and MON values for the series of 57 points (in  $\text{CDCl}_3$ ), see text for details. Reproduced from Jameel *et al.*<sup>11</sup> with the permission of the American Chemical Society.

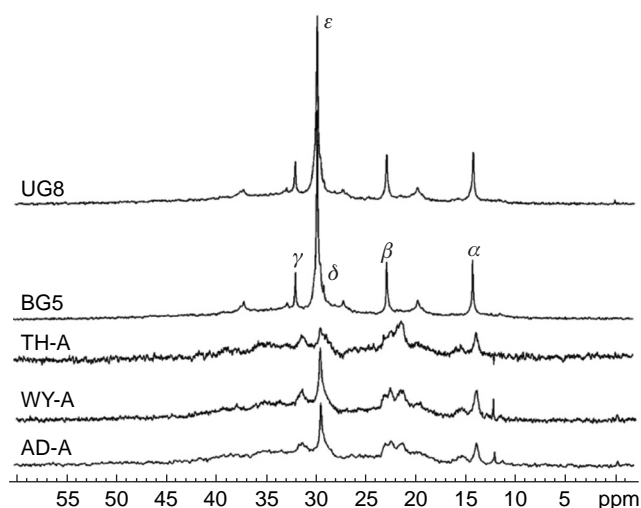


**Figure 24.** Aliphatic portion of the  $^{13}\text{C}$  NMR spectra for three neat coal-derived asphaltene samples (TH-A, WY-A, AD-A) and two petroleum asphaltenes (BG5, UG8). The peaks labeled  $\alpha$ ,  $\beta$ ,  $\gamma$ ,  $\delta$ , and  $\epsilon$  arise from terminal carbons ( $\alpha$ , 14 ppm), and carbons that are one ( $\beta$ , 22.7 ppm), two ( $\gamma$ , 32 ppm), three ( $\delta$ , 29.7 ppm), and four ( $\epsilon$ , 30.1 ppm) or more carbons away from the terminal carbon. For used abbreviations, see original text. Reproduced with minor editing privilege from Andrews *et al.*<sup>38</sup> with the permission of the American Chemical Society.

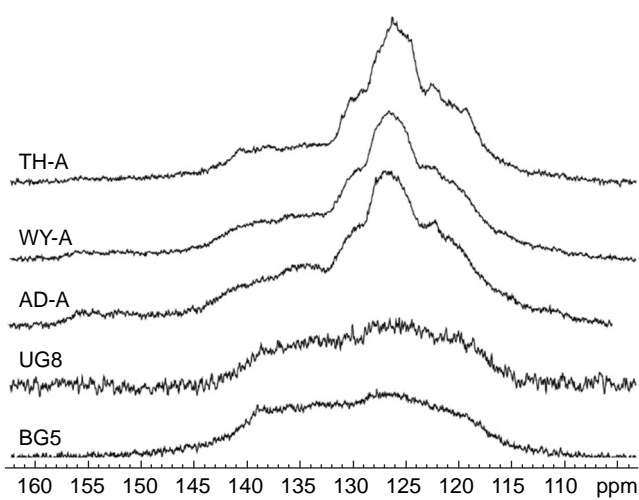


**Figure 25.** Aromatic part of the  $^{13}\text{C}$  NMR spectra for three neat coal-derived asphaltenes (TH-A, AD-A, WY-A) and two petroleum asphaltenes (BG5, UG8). The petroleum asphaltenes have roughly 50% aromatic carbons, whereas the coal-derived asphaltenes are close to 80% aromatic carbons. For used abbreviations, see original text. Reproduced with minor editing privilege from Andrews *et al.*<sup>38</sup> with the permission of the American Chemical Society.

cycloalkanes, aromatic hydrocarbons, and other important components of crude oil.

In a recent publication, Gao and coauthors<sup>40</sup> investigated crude oil from the Eocene Shahejie Formation in Lake Dongpu Sag, China by means of  $^1\text{H}$  and  $^{13}\text{C}$  NMR. Figures 29 and 30 taken from this publication provide  $^1\text{H}$  and  $^{13}\text{C}$  NMR typical spectra of crude oils from that source, accordingly. The crude oils studied are kerogens (a complex mixture of organic chemical compounds that make up the most abundant fraction of organic matter in sedimentary rocks).

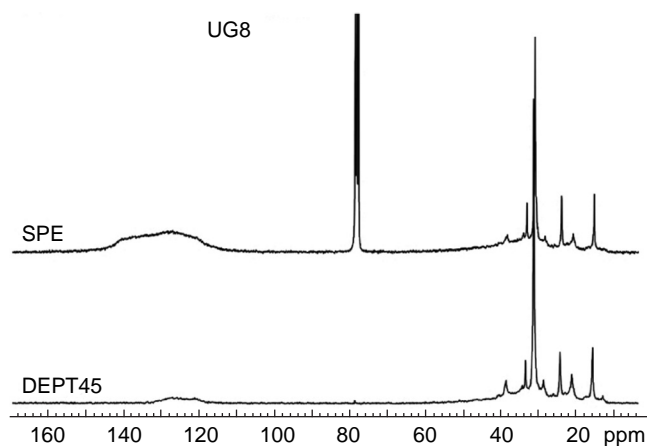


**Figure 26.** Comparison of the normal quantitative  $^{13}\text{C}$  SPC and DEPT45 spectra for the neat petroleum asphaltene sample UG8. Quantitative SPC underestimates the bridgehead carbon by 50–90%. Reproduced with minor editing privilege from Andrews *et al.*<sup>38</sup> with the permission of the American Chemical Society.

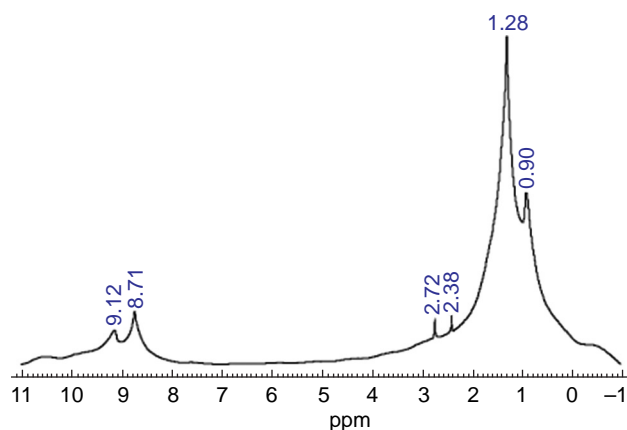


**Figure 27.** The  $^1\text{H}$  NMR spectrum of a neat asphaltene derived from Algerian Hassi Messaoud oil field recorded at 300.13 MHz in  $\text{CDCl}_3$ . Reproduced from Fergoug and Bouhadda<sup>39</sup> with the permission of Elsevier.

It was found that the types of hydrogen atoms in the crude oils studied were mainly  $\beta$  and  $\gamma$  hydrogens ( $\text{H}_\beta$  and  $\text{H}_\gamma$ , respectively), and the contents of  $\alpha$  hydrogens ( $\text{H}_\alpha$ ) and alkene hydrogens ( $\text{H}_{\text{C}=\text{C}}$ ) were very low, as illustrated in Fig. 29. In this case, the predominant carbon atom type was saturated carbon, with a smaller contribution from aromatic and heteroatomic carbons (see Fig. 30). The hydrogen types  $\text{H}_\gamma$  and  $\text{H}_\beta$  were found to be more sensitive to the organic matter source than carbons. High  $\text{H}_\gamma$  values indicated that studied crude oil was rich in polysubstituted alkanes, and its organic matter source was algae. On the other hand, high  $\text{H}_\beta$  values indicated that studied crude oil had a high wax content, and its organic matter source was the higher plants.

A general conclusion formulated by the authors<sup>40</sup> was that with increasing input of aquatic organisms,  $\text{H}_\gamma$  and methyl carbon in the chemical structure of the crude oil increased, while  $\text{H}_\beta$  decreased. Here,  $^1\text{H}$  NMR spectra were more useful than  $^{13}\text{C}$  NMR spectra in elucidating the sources of organic matter. Specifically, the principal finding of the study was that ‘NMR parameters reflect the source rock depositional environment, and organic matter source and thermal maturity.  $^1\text{H}$  NMR spectroscopy is a fast analytical method, but it provides little

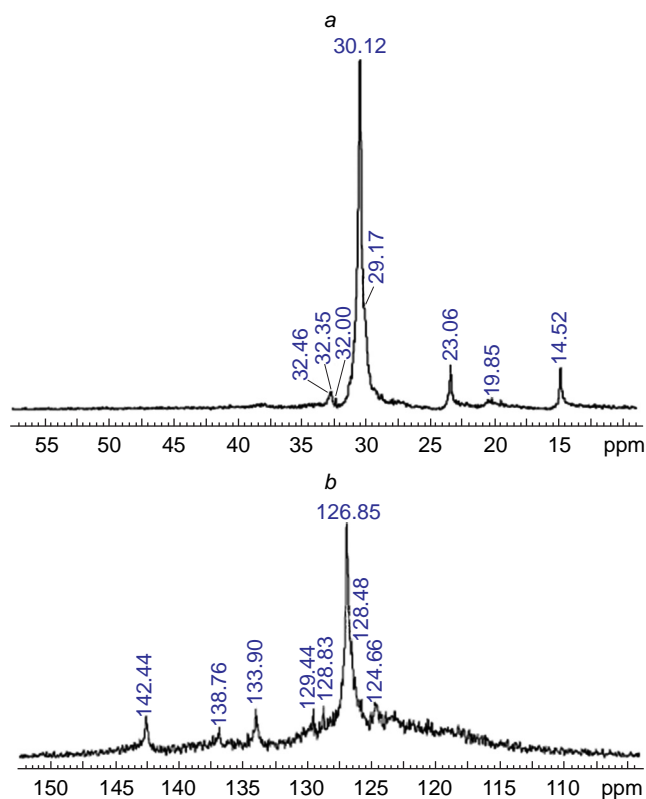


**Figure 28.** The  $^{13}\text{C}$  NMR spectrum of a neat asphaltene derived from Algerian Hassi Messaoud oil field recorded at 75.47 MHz in  $\text{CDCl}_3$  showing (a) aliphatic and (b) aromatic regions. Reproduced with minor editing privilege from Fergoug and Bouhadda<sup>39</sup> with the permission of Elsevier.

**Table 5.** Typical ranges of  $^1\text{H}$  NMR chemical shifts of functional groups defining the composition of asphaltenes. Compiled from Ok and Mal.<sup>37</sup>

Shift range, ppm	Functional group(s)
0.50–1.00	<i>t</i> - $\text{CH}_3$ on aliphatic chain
1.00–1.50	Paraffinic hydrogen, $\beta$ to aromatic carbons
1.50–2.00	alicyclic $\text{CH}_2$ and aliphatic chain $\text{CH}_2$ , respectively
2.20–2.60	$\text{CH}_3$ attached to aryl rings
2.80–3.00	Aliphatic chain/cyclic $\text{CH}_2$ alpha or beta to aromatics
3.30–3.50	$\text{CH}_2$ , $\text{CH}$ alpha to aromatic rings under steric strain
3.50–5.00	Naphthenic and porphyrinic $\text{CH}/\text{CH}_2$ groups
6.00–7.00	Monoaromatic protons
7.00–8.00	Diaromatic protons
8.00–8.50	Some tetra-, tri-, and diaromatic protons
8.50–9.40	Aromatic protons in sterically hindered positions in angular polycyclic aromatic hydrogens or next to heteroatoms or H–N
9.40–10.60	NiCHO (porphyrin)
9.00–12.00	Aldehydic and carboxylic hydrogen

information about chemical structure. In contrast,  $^{13}\text{C}$  NMR spectroscopy can provide more information regarding chemical structure.  $^1\text{H}$  NMR spectroscopy is more useful for evaluation of the organic matter source, whereas  $^{13}\text{C}$  NMR spectroscopy is more useful for the evaluation of organic matter thermal

**Table 6.** Typical ranges of  $^{13}\text{C}$  NMR chemical shifts of functional groups defining the composition of asphaltenes. Compiled from Ok and Mal.<sup>37</sup>

Shift range, ppm	Functional group(s)
11.00–18.00	Terminal $\text{CH}_3$ on aliphatic chain with at least 3 or more carbons
18.00–20.00	Branched $\text{CH}_3$ , $\alpha$ or more from terminal $\text{CH}_3$
20.00–22.00	$\text{CH}_3$ substituent on aryl ring
22.00–24.00	Terminal isobutyl $\text{CH}_3$ ; and possible $\text{CH}_2$ $\alpha$ to terminal $\text{CH}_3$
24.00–25.00	Alicyclic ring beta to aromatic ring
25.00–29.70	Aliphatic chain $\text{CH}_2$ positioned more than $\alpha$ or $\beta$ to aromatic ring
29.90–31.90	Alicyclic $\text{CH}_2$ (naphthenic)
32.00	$\text{CH}_2$ beta to <i>t</i> - $\text{CH}_3$ or aromatic ring
32.80	Aliphatic CH
33.00–39.50	$\text{CH}_2$ or CH $\alpha$ to aromatic ring, $\text{CH}_2$ $\alpha$ to branch point in chain
40.00–55.00	$\alpha$ carbon to carboxylic group (porphyrins)/ alicyclic (naphthenic) $\text{CH}/\text{CH}_2$
60.00–78.00	Paraffinic and naphthenic carbon $\alpha$ to OH
110.00–120.00	Aromatic carbons
121.00–124.00	Bay type carbons
125.00–129.00	Fjord type carbons
122.90	Riple bridgehead (peri-condensed) quaternary aromatic carbon
127.00	Aromatic protonated carbon
136.40	Double bridgehead (cata-condensed) and substituted quaternary aromatic carbon
137.00–140.50	$\alpha$ carbon to sulfur or nitrogen atom in benzo, dibenzothiophene type structures
137.00–160.00	Aromatic carbons without any proton
160.00–175.00	Ester or amide carboxy carbon atom
178.00–190.00	Quinolinic carbons
190.00–220.00	Aldehydic and ketonic carbons

maturity... NMR analysis can constrain the chemistry of crude oil, particularly the composition of functional groups<sup>7,40</sup>

Recently a series of papers have been published by Rakhmatullin and coauthors dealing with qualitative and quantitative analysis of oil samples based on NMR data, see two

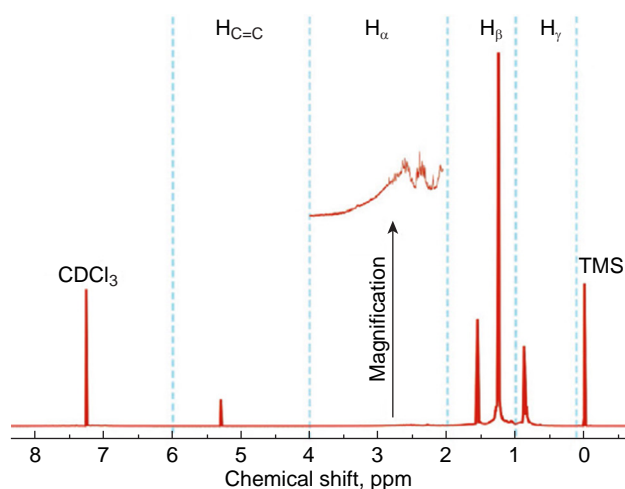


**Figure 29.** Typical  $^1\text{H}$  NMR spectrum of the analyzed kerogens in  $\text{CDCl}_3$ . Reproduced with minor editing privilege from Gao *et al.*<sup>40</sup> with the permission of Elsevier.

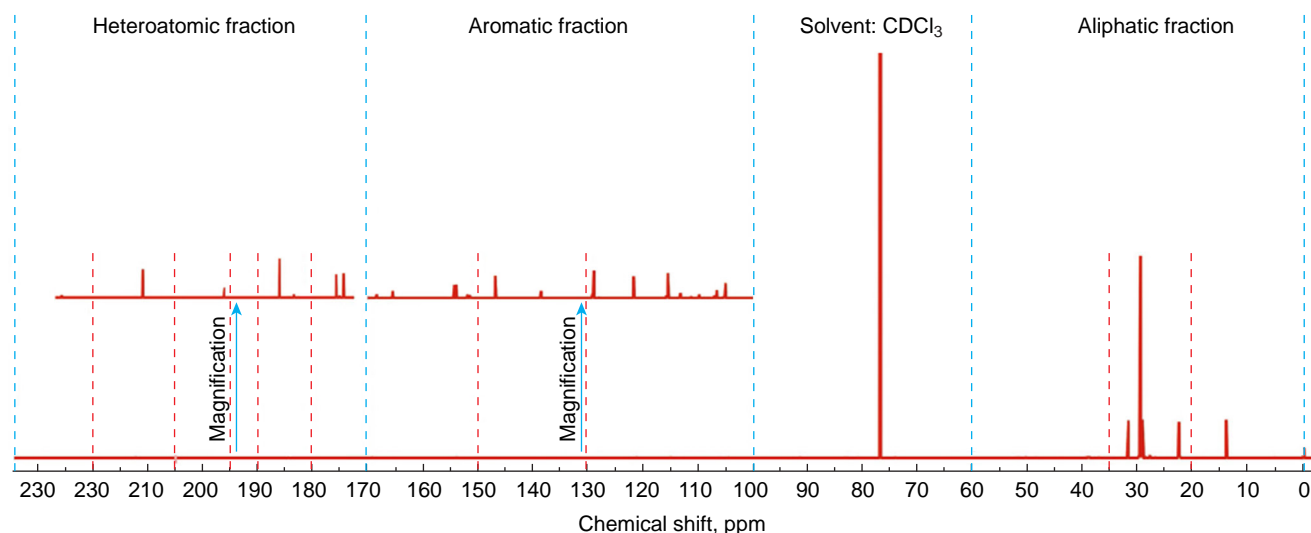
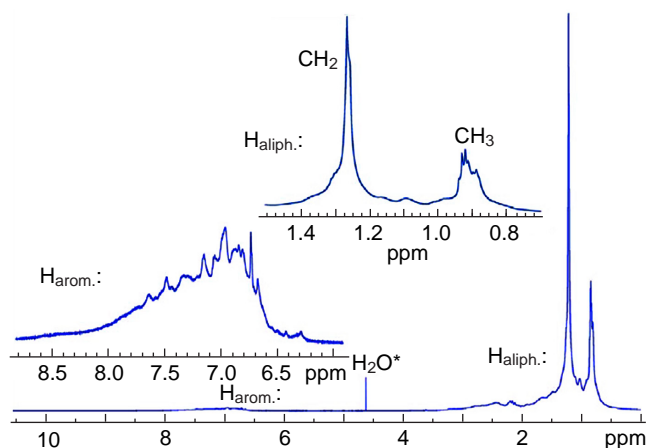


**Figure 30.** Typical  $^{13}\text{C}$  NMR spectrum of the analyzed kerogens in  $\text{CDCl}_3$ . Reproduced with minor editing privilege from Gao *et al.*<sup>40</sup> with the permission of Elsevier.

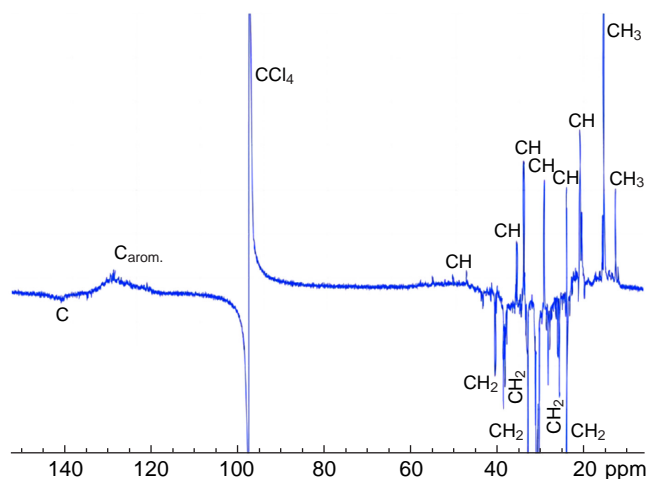
very recent reviews.<sup>41,42</sup> In one of the first publications<sup>43</sup> from this series, the authors recorded representative  $^1\text{H}$  and  $^{13}\text{C}$  NMR spectra of the crude oil samples from Bashkortostan and Tatarstan oilfields using a 700 MHz spectrometer. The representative  $^1\text{H}$  and  $^{13}\text{C}$  NMR spectra taken from that publication are provided in Figs 31–33. On the basis of these data, the quantitative fractions of aliphatic and aromatic molecules (tertiary and primary carbon atoms, aromatic rings, olefins), together with the functional groups constituting oil hydrocarbons were determined and their variation from sample to sample of particular geographical origin was analyzed.

Figure 31 provides some interesting details in the  $^1\text{H}$  NMR spectrum of the selected oil sample recorded at 700 MHz which are not present in the lower-field NMR spectra. For example, the multiple individual methyl signals can be distinguished in the region of 0.8–1.0 ppm. It means that the studied oil sample contains hydrocarbon chains of several different types, each having its own set of terminal methyl groups.

The HSQC  $^{13}\text{C}$  NMR spectrum of the same oil sample is shown in Fig. 32. This experiment made it possible to distinguish



**Figure 31.**  $^1\text{H}$  NMR spectrum (700 MHz) of oil sample from the top of Bashkirian oil well (Akansk field) in  $\text{CCl}_4$  (inserts show zoomed signals of aromatic and aliphatic protons). Residual water signal in the capillary is marked with asterisk. Reproduced from Rakhmatullin *et al.*<sup>43</sup> with the permission of Elsevier.



**Figure 32.** The HSQC  $^{13}\text{C}$  NMR spectrum (176 MHz) of oil sample from the top of Bashkirian oil well (Akansk field) in  $\text{CCl}_4$ . Reproduced from Rakhmatullin *et al.*<sup>43</sup> with the permission of Elsevier.

primary and tertiary carbons from the secondary and quaternary carbons. Generally, if a  $^{13}\text{C}$  atom is bound to an odd number of protons, a positive signal is observed; in the case of an even number of protons, the negative peaks appear. It allows the assignment of corresponding signals in the overlapping areas of CH and  $\text{CH}_2$  resonances.

Some additional information was provided by the two-dimensional  $^1\text{H}$ – $^{13}\text{C}$  HSQC NMR spectra exemplified for the same sample in Fig. 33. However, low digital resolution in both dimensions and rapid decay of the NMR signals are the main drawbacks of using 2D NMR technique in petroleum chemistry. As an example of these disadvantages, individual signals in the highfield region (0.5–2 ppm in the  $^1\text{H}$  and 20–50 ppm in the  $^{13}\text{C}$  NMR spectra) are difficult to distinguish.

In the next publication Rakhmatullin and coauthors<sup>44</sup> used  $^1\text{H}$  and  $^{13}\text{C}$  NMR to study three samples of light paraffinic crude oil and one sample of heavy aromatic crude oil, namely two samples of the Middle–Nazym oilfield (Russia, viscosity 5.95 and 7.5  $\text{mPa}\cdot\text{s}$ ), a sample from the Vishanskoe oilfield (Belarus, viscosity 37.2  $\text{mPa}\cdot\text{s}$ ), and a heavy sample from the Ashal'cha

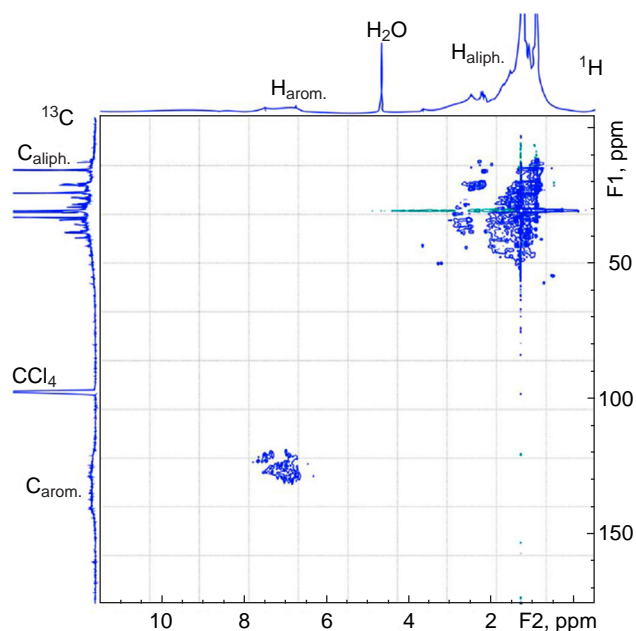


**Figure 33.** The two-dimensional  $^1\text{H}$ - $^{13}\text{C}$  HSQC NMR spectrum (700 MHz) of oil sample from the top of Bashkirian oil well (Akansk field) in  $\text{CCl}_4$ . Reproduced from Rakhmatullin *et al.*<sup>43</sup> with the permission of Elsevier.

oilfield (Tatarstan, viscosity 2.420  $\text{mPa}\cdot\text{s}$ ). The representative  $^1\text{H}$  and  $^{13}\text{C}$  NMR spectra recorded at 500 and 700 MHz for protons (126 and 176 MHz for carbons, accordingly) are shown in Figs 34–37. In the last two figures from this series, the samples of crude oil were taken from the Middle–Nazym oilfield, Russia (1, 2); the Vishanskoe oilfield, Belarus (3); and the Ashal’cha oilfield, Tatarstan (4). In that paper, the quantitative fractions of aromatic molecules and functional groups constituting oil hydrocarbons were determined, and a comparative analysis of the oil samples of different viscosity and origin was performed.

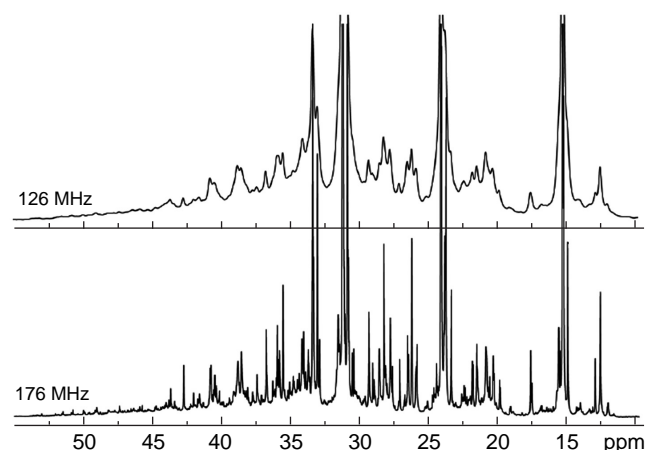


**Figure 35.**  $^{13}\text{C}$  NMR spectra (aliphatic region) of the Middle–Nazym oilfield sample (Russia, viscosity 7.5  $\text{mPa}\cdot\text{s}$ ) at 126 and 176 MHz in  $\text{CCl}_4$ . Reproduced from Rakhmatullin *et al.*<sup>44</sup> under the CC BY-NC 4.0 International Public License.

In the next paper in the series, Rakhmatullin and coauthors<sup>45</sup> examined in the same way three low-viscosity light, one semi-heavy, and two high-viscosity crude oils samples provided by Tatneft, Zarubezhneft and RITEK oil companies (Russia). Quantitative fractions of aromatic molecules and functional groups constituting oil hydrocarbons were determined by means of  $^1\text{H}$  and  $^{13}\text{C}$  NMR spectroscopy, and comparative analysis of the oil samples with different viscosity, origin and preliminary treatment was carried out. Representative  $^1\text{H}$  and  $^{13}\text{C}$  NMR spectra (recorded at 500 and 125 MHz, accordingly) are shown in Figs 38 and 39.

As a follow-up to these studies, the same principal authors<sup>46</sup> examined four different heavy oil samples of different geographical origin with the viscosities ranging from 100 to 50000  $\text{mPa}\cdot\text{s}$ , as specified in Table 7. The presence of all major hydrocarbon components, both in crude oil and in each of its fractions, was established quantitatively by using  $^{13}\text{C}$  NMR spectroscopy. The  $^{13}\text{C}$  NMR spectra of crude oils 1–4 and their

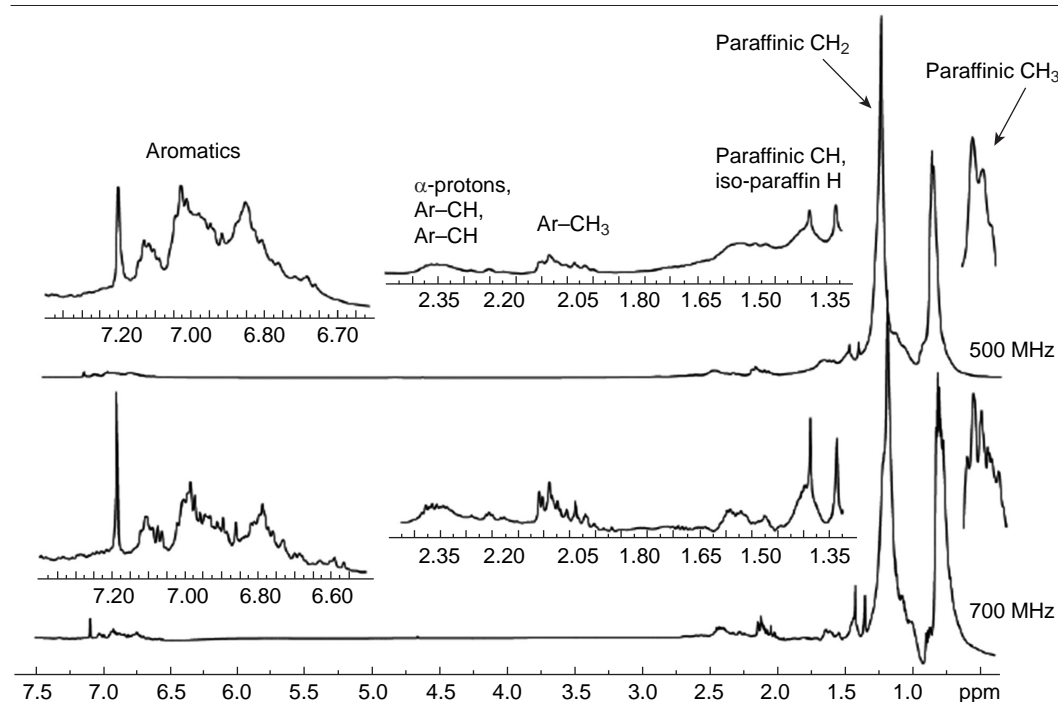


**Figure 34.**  $^1\text{H}$  NMR spectra of the Middle–Nazym oilfield sample (Russia, viscosity 7.5  $\text{mPa}\cdot\text{s}$ ) at 500 and 700 MHz in  $\text{CCl}_4$ . Reproduced from Rakhmatullin *et al.*<sup>44</sup> under the CC BY-NC 4.0 International Public License.

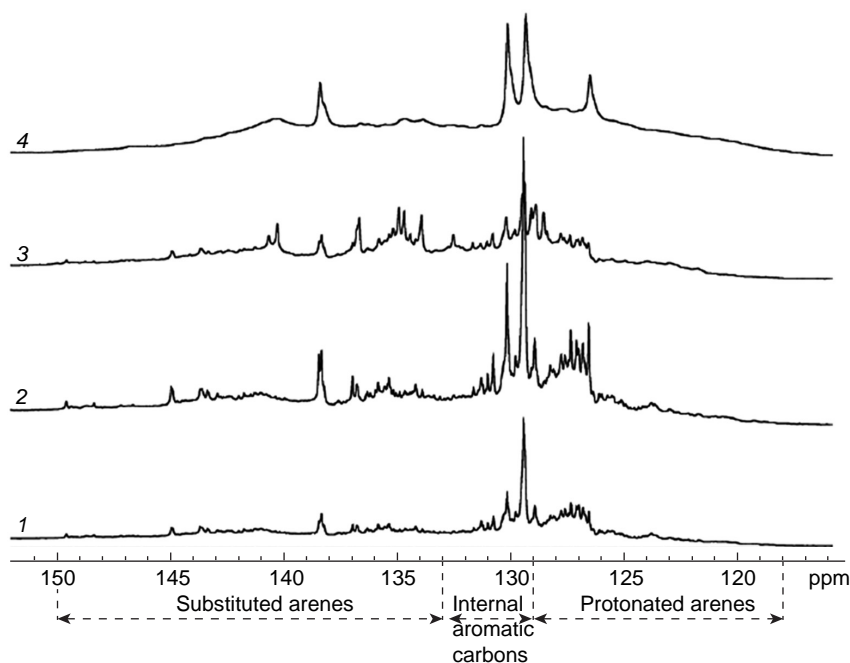


**Figure 36.** The aromatic region of the  $^{13}\text{C}$  NMR spectra (176 MHz,  $\text{CCl}_4$ ) of the Middle–Nazym oilfield sample (Russia, viscosity 7.5  $\text{mPa}\cdot\text{s}$ ) (1); the Middle–Nazym oilfield sample (Russia, viscosity 5.95  $\text{mPa}\cdot\text{s}$ ) (2); the Vishanskoe oilfield sample (Belarus, viscosity 37.2  $\text{mPa}\cdot\text{s}$ ) (3); the Ashal’cha oilfield sample (Tatarstan, viscosity 2420  $\text{mPa}\cdot\text{s}$ ), (4). Reproduced from Rakhmatullin *et al.*<sup>44</sup> under the CC BY-NC 4.0 International Public License.

**Table 7.** Studied oil samples and their viscosities. Compiled from Rakhmatullin *et al.*<sup>46</sup>

Sample	Viscosity, $\text{mPa}\cdot\text{s}$	Geographical origin
1	106	Iraq
2	1430	Turkmenistan
3	2420	Tatarstan
4	49700	Cuba

fractions (saturated compounds, aromatics, resins, and asphaltenes) studied in that paper are shown in Fig. 40 and 41, accordingly, while calculated molar fractions of primary, secondary and quaternary, tertiary, and aromatic carbons, together with aromaticity factor and mean chain length of aliphatic hydrocarbons are shown in Table 8.

It can be seen that the oil sample from Cuba, in contrast to the other three samples from Iraq, Turkmenistan, and Tatarstan, had the lowest content of secondary and quaternary carbons (36.6%) and the highest content of aromatic carbons (27.5%) resulting in the highest value of aromaticity factor (0.275).

Based on the results of that study,<sup>46</sup> authors concluded that generally,  $^{13}\text{C}$  NMR spectroscopy could significantly expand the ‘repertoire’ (the word in quotation marks is taken from the original text) of the research methods to study structural-group composition of oil and oil fractions. It also adequately described, qualitatively and quantitatively, not only the elemental

**Table 8.** Molar fractions (%) of primary ( $C_p$ ), secondary and quaternary ( $C_{sq}$ ), tertiary ( $C_t$ ), and aromatic ( $C_{ar}$ ) carbons, together with aromaticity factor (FCA), and average chain length (ACL) of aliphatic hydrocarbons based on the analysis of  $^{13}\text{C}$  NMR spectra of samples 1–4. Compiled from Rakhmatullin *et al.*<sup>46</sup>

Parameter	1	2	3	4
$C_p$	25.8	18.8	21.6	18.8
$C_{sq}$	53.0	52.6	48.9	36.6
$C_t$	10.0	13.9	12.8	15.1
$C_{ar}$	12.5	14.7	19.3	27.5
FCA	0.123	0.147	0.188	0.275
ACL	6.9	9.1	7.7	7.7

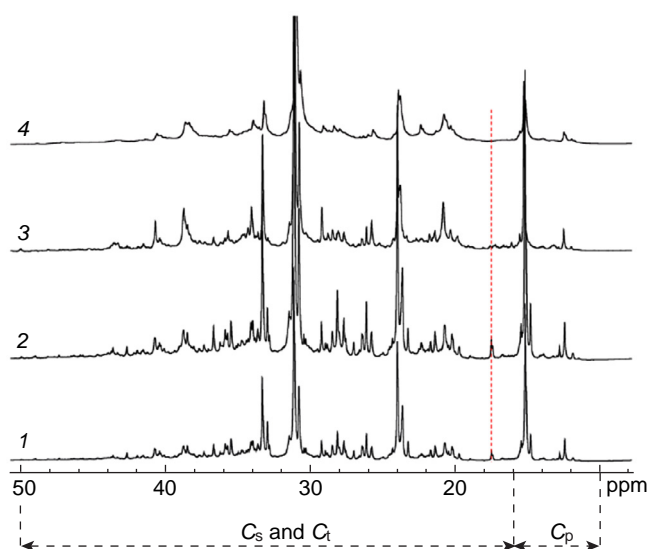


**Figure 37.** The aliphatic region of the  $^{13}\text{C}$  NMR spectra (176 MHz,  $\text{CCl}_4$ ) of the Middle–Nazym oilfield sample (Russia, viscosity 7.5  $\text{mPa}\cdot\text{s}$ ) (1); the Middle–Nazym oilfield sample (Russia, viscosity 5.95  $\text{mPa}\cdot\text{s}$ ) (2); the Vishanskoe oilfield sample (Belarus, viscosity 37.2  $\text{mPa}\cdot\text{s}$ ) (3); the Ashal’cha oilfield sample (Tatarstan, viscosity 2420  $\text{mPa}\cdot\text{s}$ ), (4).  $C_p$ ,  $C_s$ , and  $C_t$  stand accordingly, for primary, secondary, and tertiary carbons. Reproduced from Rakhmatullin *et al.*<sup>44</sup> under the CC BY-NC 4.0 International Public License.

composition of oil samples 1–4, but also the molecular structures of the related natural organic material, its fractions, and intermediate and target products. It was also demonstrated that the high-field  $^{13}\text{C}$  NMR spectroscopy made it easy to establish the quantitative presence of the main hydrocarbon components in the main oil fractions including saturated compounds, aromatics, resins, and asphaltenes.

In a more detailed  $^1\text{H}$  and  $^{13}\text{C}$  NMR study of the crude oil from the Cuban oilfield and the oil-containing rock samples from the Cuban basin listed in Table 9, Rakhmatullin *et al.*<sup>47</sup> studied the composition of various structural fragments of these

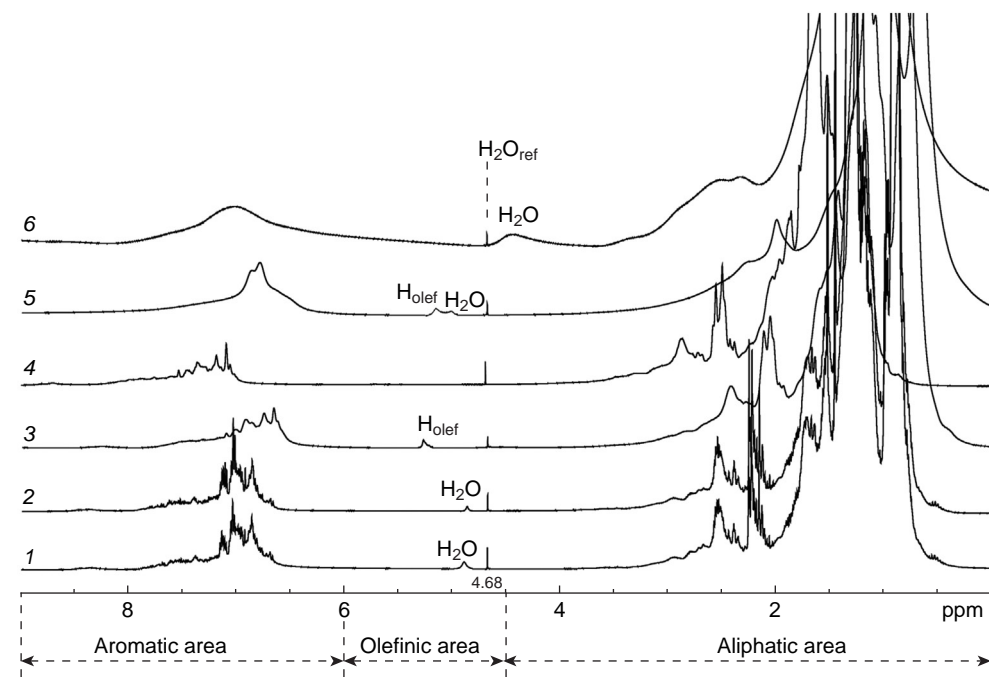


**Figure 38.**  $^1\text{H}$  NMR spectra (500 MHz,  $\text{CCl}_4$ ) of the following crude oil samples: 1 — high pressure air injection (viscosity  $7.5 \text{ mPa}\cdot\text{s}$ ), 2 — primary recovery (viscosity  $5.95 \text{ mPa}\cdot\text{s}$ ), 3 — high pressure air injection (viscosity  $37.2 \text{ mPa}\cdot\text{s}$ ), 4 — primary recovery (viscosity  $106 \text{ mPa}\cdot\text{s}$ ), 5 — steam-assisted gravity drainage (viscosity  $2420 \text{ mPa}\cdot\text{s}$ ), 6 — cyclic steam stimulation (viscosity  $49700 \text{ mPa}\cdot\text{s}$ ). Reproduced from Rakhmatullin *et al.*<sup>45</sup> with the permission of Elsevier.

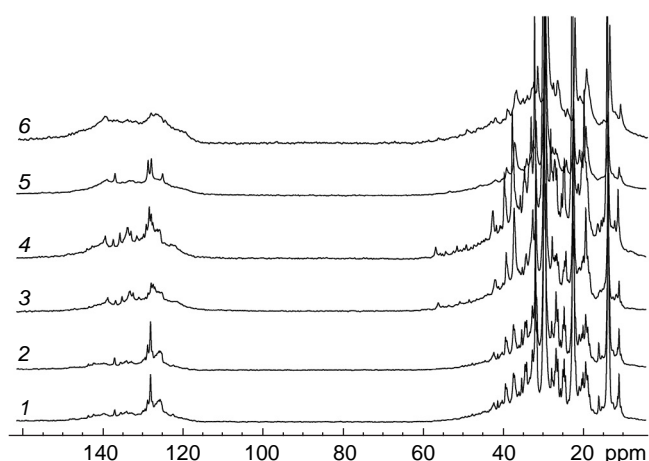


**Figure 39.**  $^{13}\text{C}$  NMR spectra (125 MHz,  $\text{CCl}_4$ ) of the following crude oil samples: 1 — high pressure air injection (viscosity  $7.5 \text{ mPa}\cdot\text{s}$ ), 2 — primary recovery (viscosity  $5.95 \text{ mPa}\cdot\text{s}$ ), 3 — high pressure air injection (viscosity  $37.2 \text{ mPa}\cdot\text{s}$ ), 4 — primary recovery (viscosity  $106 \text{ mPa}\cdot\text{s}$ ), 5 — steam-assisted gravity drainage (viscosity  $2420 \text{ mPa}\cdot\text{s}$ ), 6 — cyclic steam stimulation (viscosity  $49700 \text{ mPa}\cdot\text{s}$ ). Reproduced from Rakhmatullin *et al.*<sup>45</sup> with the permission of Elsevier.

**Table 9.** Molar fractions (%) of primary ( $C_p$ ), secondary and quaternary ( $C_{sq}$ ), tertiary ( $C_t$ ), and aromatic ( $C_{ar}$ ) carbons, together with the aromaticity factor (FCA), and the average chain length (ACL) of aliphatic hydrocarbons of the Cuban oil and oil-containing rock extractions derived from  $^{13}\text{C}$  NMR spectra. Compiled from Rakhmatullin *et al.*<sup>47</sup>

Parameter	Crude oil	Oil-containing rock extraction					
		III-5	VIII-1	VIII-3	VIII-4	VIII-5	IX-2
$C_p$	18.8	9.1	5.6	10.0	10.8	12.0	8.0
$C_{sq}$	38.6	47.8	35.4	39.6	54.1	46.2	34.8
$C_t$	15.1	12.5	11.3	14.5	12.1	12.6	20.6
$C_{ar}$	27.5	30.6	47.7	35.9	23.0	29.2	36.6
FCA	0.275	0.306	0.477	0.359	0.230	0.292	0.366
ACL	7.7	15.2	18.7	12.8	14.2	11.8	15.8

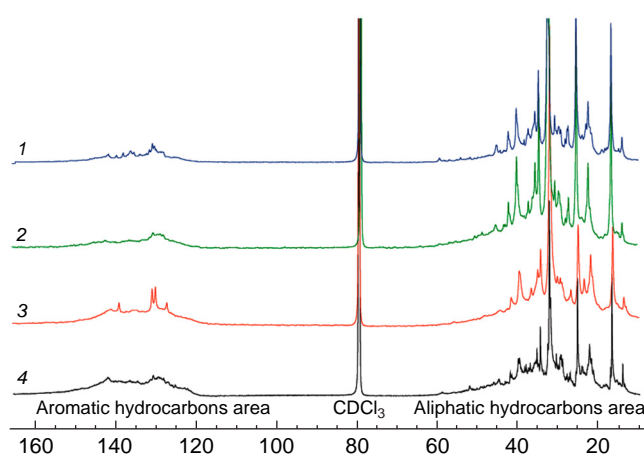


**Figure 40.**  $^{13}\text{C}$  NMR spectra (175 MHz) of oil samples 1–4 in  $\text{CDCl}_3$ . Reproduced from Rakhmatullin *et al.*<sup>46</sup> under the CC BY-NC 4.0 International Public License.

samples in the aliphatic and aromatic regions and evaluated the molar fractions of primary, secondary, quaternary, tertiary, and aromatic groups together with the aromaticity factor and the average length of the hydrocarbon chain of aliphatic hydrocarbons. The  $^1\text{H}$  and  $^{13}\text{C}$  NMR spectra of the crude oil and oil-containing rock samples investigated (five oil-containing rock samples were studied in this paper, designated III-5, VIII-1, VIII-3, VIII-4, VIII-5, and IX-2) are shown in Figs 42 and 43, respectively. These data demonstrated that their aromaticity factor and average hydrocarbon chain length were close to those of the super heavy oils.

In one of their most recent papers, Rakhmatullin *et al.*<sup>48</sup> proposed a comprehensive method for identifying signals in the  $^{13}\text{C}$  NMR spectra of crude oils exemplified with a typical crude oil sample providing 66 individual resonances in the  $^{13}\text{C}$  NMR spectrum recorded on a 700 MHz spectrometer (175 MHz for  $^{13}\text{C}$  NMR). In that study, authors used normal proton-decoupled ( $^{13}\text{C}$ ),  $^{13}\text{C}$  Attached Proton Test ( $^{13}\text{C}$  APT), and  $^{13}\text{C}$  with Gated Decoupling ( $^{13}\text{C}$  GD) modes. All characteristic signals are

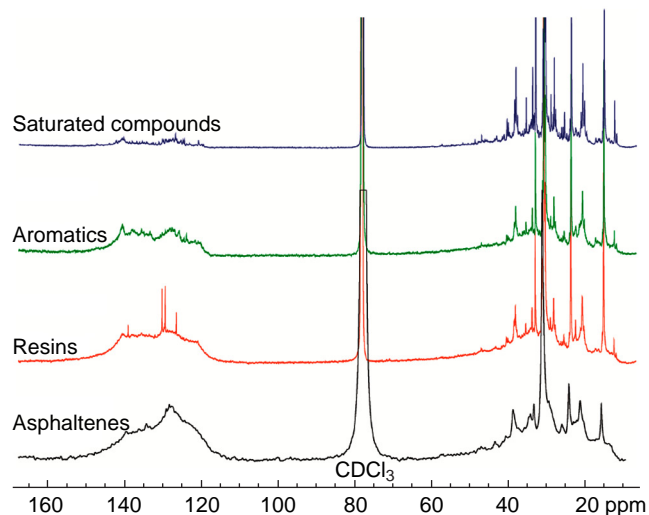


**Figure 41.**  $^{13}\text{C}$  NMR spectra (175 MHz) of the main oil fractions (saturated compounds, aromatics, resins, and asphaltenes) in  $\text{CDCl}_3$ . Reproduced with minor editing privilege from Rakhmatullin *et al.*<sup>46</sup> under the CC BY-NC 4.0 International Public License.

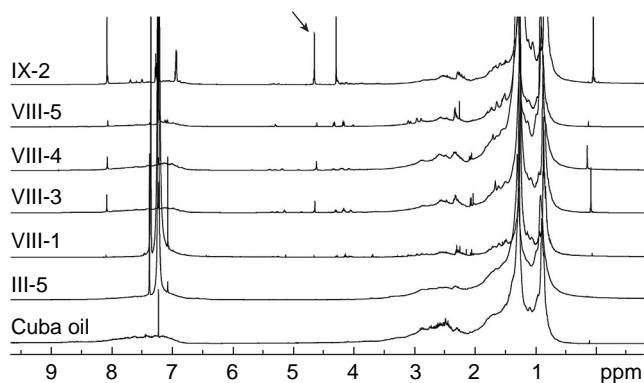


**Figure 42.**  $^1\text{H}$  NMR Spectra (700 MHz) of the Cuban oil and extracted samples from the oil-containing rocks (specified as III-5, VIII-1, VIII-3, VIII-4, VIII-5, IX-2) in  $\text{CDCl}_3$ . Reproduced from Rakhmatullin *et al.*<sup>47</sup> under the CC BY-NC 4.0 International Public License.

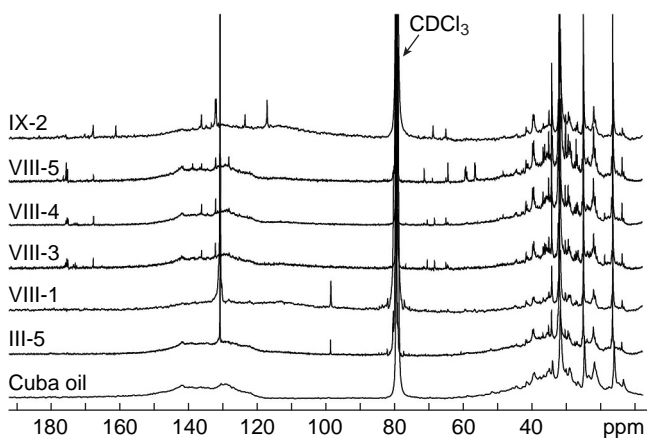


**Figure 43.**  $^{13}\text{C}$  NMR spectra (175 MHz) of the Cuban oil and extracted samples from the oil-containing rocks (specified as III-5, VIII-1, VIII-3, VIII-4, VIII-5, IX-2) in  $\text{CDCl}_3$ . Reproduced from Rakhmatullin *et al.*<sup>47</sup> under the CC BY-NC 4.0 International Public License.

**Table 10.** The detailed characterization of the  $^{13}\text{C}$  NMR spectrum of a typical oil sample (signals 1–22: aromatic area; signals 23–46: lowfield aliphatic area; signals 47–66: highfield aliphatic area). Compiled from Rakhmatullin *et al.*<sup>48</sup>

Peak No	Carbon type	Chemical shift, ppm	Peak No	Carbon type	Chemical shift, ppm
1	C	161.71	34	$\text{CH}_2$	52.24
2	C	160.90	35	$\text{CH}_2$	51.81
3	C	153.63	36	$\text{CH}_2$	51.31
4	C	151.95	37	$\text{CH}_2$	51.14
5	C	149.59	38	$\text{CH}_2$	50.24
6	C	149.09	39	$\text{CH}_2$	48.28
7	C	148.16	40	$\text{CH}_2$	47.43
8	C	143.02	41	$\text{CH}_2$	47.28
9	C	142.63	42	$\text{CH}_2$	46.95
10	C	141.57	43	$\text{CH}_2$	46.47
11	CH	134.63	44	$\text{CH}_2$	45.66
12	CH	128.89	45	$\text{CH}_2$	45.48
13	CH	128.57	46	$\text{CH}_2$	44.16
14	CH	127.87	47	$\text{CH}_2$	39.88
15	CH	127.34	48	$\text{CH}_2$	37.27
16	CH	126.26	49	$\text{CH}_2$	35.98
17	CH	125.89	50	$\text{CH}_2$	34.23
18	CH	125.73	51	$\text{CH}_2$	33.91
19	CH	122.40	52	CH	33.63
20	CH	121.60	53	CH	33.21
21	CH	121.06	54	CH	32.77
22	CH	120.26	55	$\text{CH}_2$	32.34
23	$\text{CH}_2$ or C	72.41	56	CH	31.84
24	$\text{CH}_2$ or C	71.66	57	CH	30.85
25	CH	70.00	58	CH	30.55
26	CH	68.09	59	$\text{CH}_2$	30.11
27	CH	67.61	60	$\text{CH}_2$	29.76
28	$\text{CH}_2$ or C	65.49	61	$\text{CH}_3$	28.60
29	CH	63.50	62	$\text{CH}_3$	24.90
30	CH	63.21	63	$\text{CH}_2$	23.11
31	$\text{CH}_2$	54.00	64	$\text{CH}_3$	20.12
32	$\text{CH}_2$	53.93	65	$\text{CH}_3$	14.53
33	$\text{CH}_2$	53.55	66	CH	11.83

shown in Figs 44–46, while the corresponding  $^{13}\text{C}$  NMR chemical shifts are listed in Table 10.

As was stated by one of the reviewers, ‘one can find some gaps or silences (see the absence of comments on the signal in Fig. 45 which appears unnumbered between 36 and 37), discrepancies between the chemical shifts of Table 10 with the figure (signal 36 at 51.31 ppm and signal 37 at 51.14 ppm — in the figure signal 37 appears to be at deltas less than 51)’. We leave this comment for a more thorough consideration by the readers of this review.

A general conclusion of the latter study was that ‘the use of  $^{13}\text{C}$  NMR spectroscopy to study structural-group composition of oils and oil fractions can expand the accurate methods of quantitative analysis, adequately describing not only the elemental composition, which is now of no difficulty, but also the molecular structure and supramolecular structure of natural organic material, its fractions, intermediate products and target products. NMR spectroscopy methods make it easy to establish the quantitative presence of the main hydrocarbon components in any fraction of oil. Information on the content of general functional groups obtained by  $^{13}\text{C}$  NMR spectroscopy can be useful for fast prediction of oil product properties changing upon different type of treatment’.<sup>48</sup>

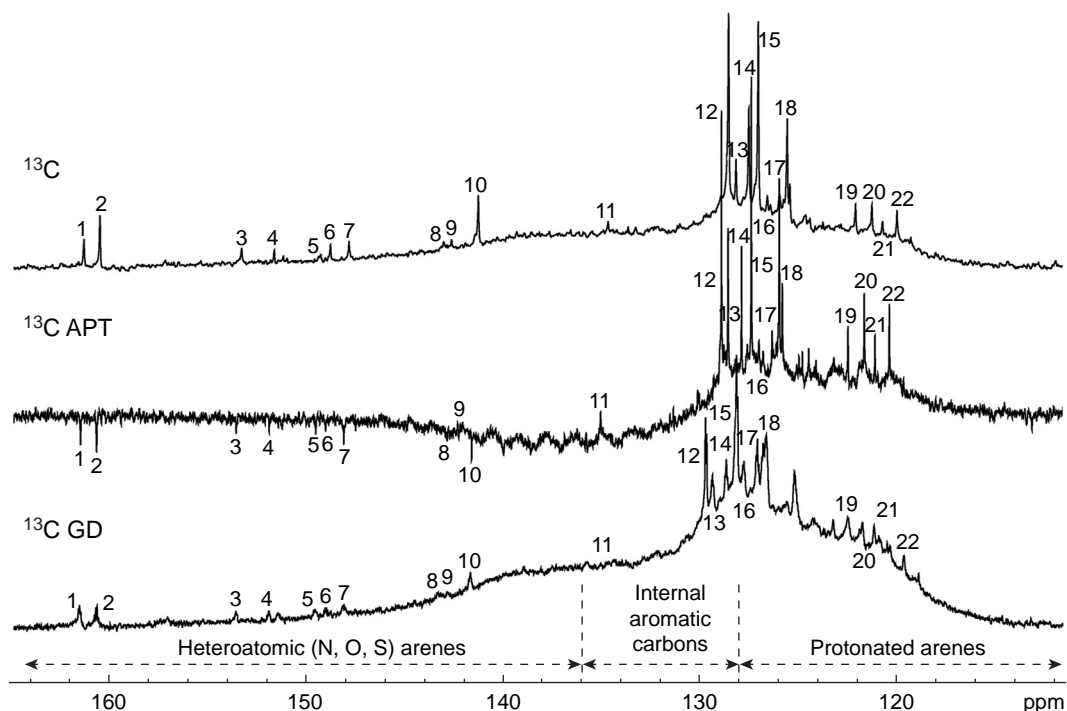


**Figure 44.** Labeling peaks in the  $^{13}\text{C}$  NMR spectra (175 MHz,  $\text{CDCl}_3$ ) of a crude oil sample (aromatic area). Reproduced from Rakhmatullin *et al.*<sup>48</sup> under the CC BY-NC 4.0 International Public License.

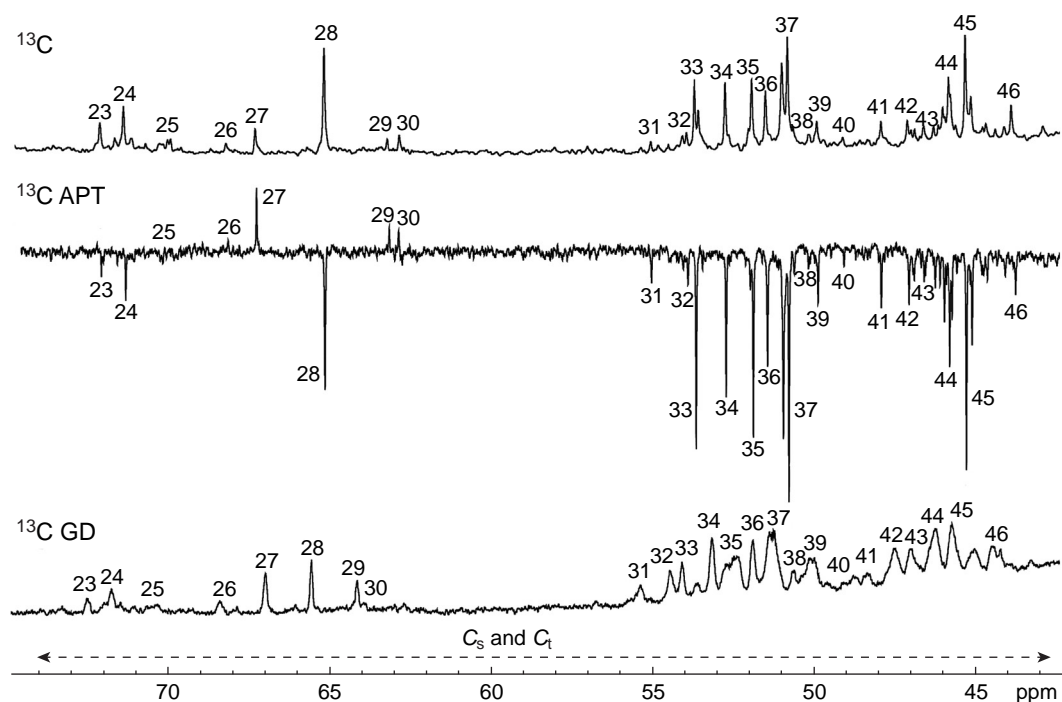


**Figure 45.** Labeling peaks in the  $^{13}\text{C}$  NMR spectra (175 MHz,  $\text{CDCl}_3$ ) of a crude oil sample (lowfield aliphatic area). Reproduced from Rakhmatullin *et al.*<sup>48</sup> under the CC BY-NC 4.0 International Public License.

### 3. Conclusion

The latest achievements in the NMR studies of oil and oil refining products reviewed are at the cutting edge of modern oil refining chemistry and petrochemical industry.

**Light fractions.** In general, there is an overwhelming number of publications dealing with NMR applications to the structural

elucidation of gasoline, light naphthas and their fractions.  $^1\text{H}$  and  $^{13}\text{C}$  NMR are also used in fuel industry to estimate reservoir properties such as porosity, permeability, wettability, irreducible water saturation, and irreducible oil saturation. In fact, the exploration and production of oil-refining products essentially benefited from the NMR application to the evaluation of oil-refining products.

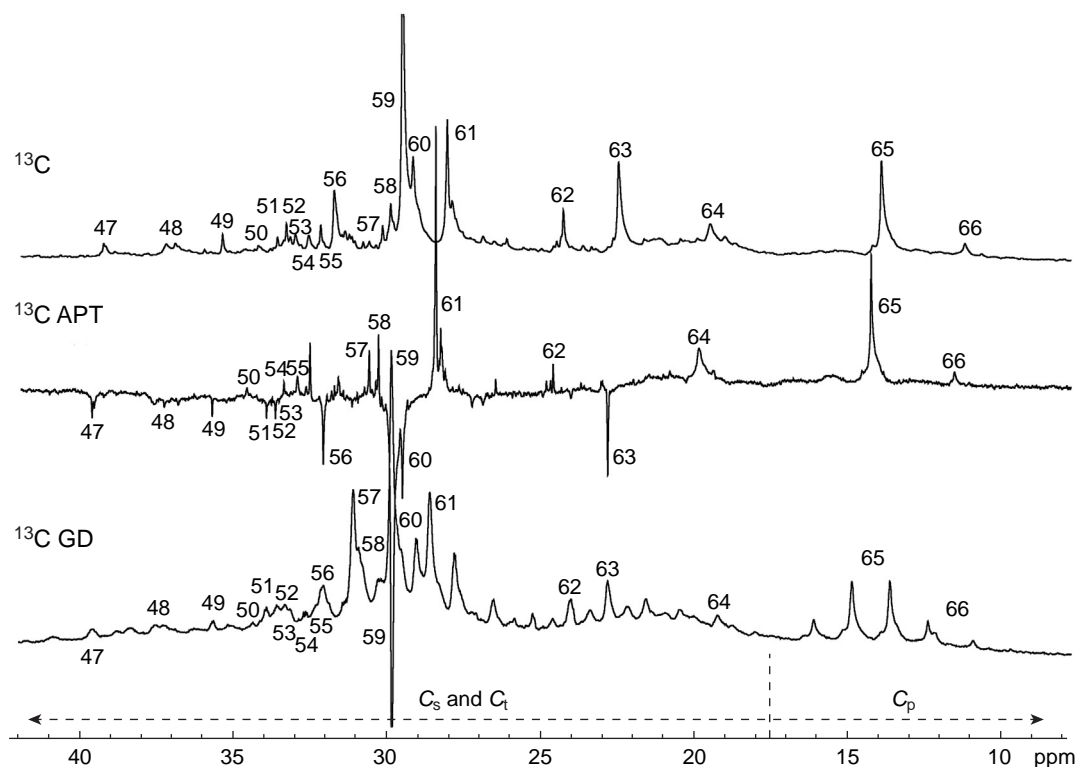


**Figure 46.** Labeling peaks in the  $^{13}\text{C}$  NMR spectra (175 MHz,  $\text{CDCl}_3$ ) of a crude oil sample (highfield aliphatic area). Reproduced from Rakhmatullin *et al.*<sup>48</sup> under the CC BY-NC 4.0 International Public License.

Much structural information is provided by the  $^1\text{H}$  and  $^{13}\text{C}$  NMR spectra of naphthas, *i.e.* the mixtures consisting mainly of aliphatic hydrocarbons, predominantly the open-chain and cyclic pentane and hexane derivatives. The application of NMR spectroscopy to the structural elucidation of naphthas has enabled a number of structural applications, in particular the following:

- determination of gasoline octane number based on the correlation between octane number and chemical composition of fluid catalytic cracking gasoline;

- determination of the composition of aromatics, naphthenes, and paraffins in straight run gasoline fractions;

- performing quantitative analysis of naphthene and isoparaffin mixtures consisting of different types of cycloalkane molecules with boiling points in the gasoline range together with a rapid and accurate quantitative determination of the composition and quality of different gasolines;

- development of a direct and fast method based on the  $^1\text{H}$  NMR spectroscopy for the determination of paraffins, olefins, naphthenes, and aromatics;

- development of an improved model for predicting the quality of hydrocarbon fuels by means of  $^1\text{H}$  NMR using a calibration set of cetane numbers of pure hydrocarbons and hydrocarbon blends of known composition;

- development of a novel approach to the analysis of light naphthas by means of the NMR spectra of five key structural groups, namely paraffinic  $\text{CH}_3$ ,  $\text{CH}_2$ , and  $\text{CH}$ , naphthenic  $\text{CH}-\text{CH}_2$ , and aromatic  $\text{C}-\text{CH}$ ;

- development of a powerful method for the accurate determination of quaternary, methine, methylene, and methyl carbons together with the identification of conjugated diolefins in gasolines by two-dimensional NMR techniques.

**Fuels.** Straight run diesels, a representative example of fuels, are characterized by a narrow distribution of aromatics, while

naphthenic diesels display a wide unresolved ‘hump’ in the aliphatic carbon region, which can be attributed to the fraction of naphthenic and paraffinic carbons. The DEPT technique allows methyl, methylene, methane, and quaternary carbons of fuels to be observed separately in the  $^{13}\text{C}$  NMR spectra, providing an average aromatic ring size and other important average molecular parameters, so that the whole refinery processing can be monitored. The use of the HSQC method allows for the determination of the fuel-specific integral regions in the  $^{13}\text{C}$  NMR spectra of diesel fuels together with the identification of overlapping peaks. Here, important information can be obtained from the  $^{13}\text{C}$  NMR spectra of diesel fuels, such as average chain length, alkyl substitution, aromatic carbon distribution, *iso*-paraffinic content, and branching index together with the branching structures of *iso*-paraffins and related hydrocarbons. NMR spectroscopy combined with artificial neural networks makes it possible to predict two of the most commonly employed octane ratings of diesel fuels, namely the research octane numbers and the motor octane numbers.

**Asphaltenes.** Asphaltenes, a complex natural mixture of organic compounds together with chemically incorporated metal complexes, consist of aromatic cores bonded to aliphatic and aromatic molecules containing heavy metals. NMR spectroscopy is widely used to characterize the chemical structure of asphaltenes and to describe their chemical behavior. Only protonated carbons are usually observed in the DEPT spectra of asphaltenes. The average structure of asphaltenes contains seven condensed aromatic rings attached to each other by short aliphatic chains of 4 to 6 carbons, as shown by both  $^1\text{H}$  and  $^{13}\text{C}$  NMR spectra. It was established that the coal-derived asphaltenes were essentially smaller than those of the original petroleum asphaltenes. Herein, the interior bridgehead carbons are an important component of asphaltenes correctly accounting for the number of fused rings in the sample. Significantly longer

chains of at least 9 carbons are characteristic of petroleum asphaltenes, as compared to the coal-derived asphaltenes.

**Crude oil.** NMR spectroscopy is widely used for the structural elucidation of natural organic materials like crude oil and oil-refining products, essentially extending the limits of other physical methods. It is useful for rapid and robust prediction of oil properties adequately describing not only the composition, but also the molecular and supramolecular structure of crude oil, its fractions, and oil-processing products. Generally,  $^{13}\text{C}$  NMR spectroscopy could significantly expand the applicability of the research methods to study the structural-group composition of oil and oil fractions. High-field  $^{13}\text{C}$  NMR spectroscopy makes it easy to quantitatively determine the presence of the main hydrocarbon components in the main oil fractions including saturated compounds, aromatics, resins, and asphaltenes. NMR has unique advantages in the geochemical analysis of crude oil because it can provide extensive information on the general chemical structure including the specification of functional groups in aliphatic hydrocarbons, cycloalkanes, aromatic hydrocarbons as well as the composition of functional groups and other important components of crude oil.  $^{13}\text{C}$  NMR normal proton-decoupled, attached proton test, and gated decoupling modes together with two-dimensional pulse methods like COSY, NOESY (Nuclear Overhauser effect Spectroscopy), and ROSY (Relaxation Ordered Spectroscopy) together with many others are widely used to determine tertiary and primary carbon atoms, aromatic rings, and olefins. As an illustrative example, the HSQC experiment allows primary and tertiary carbons to be distinguished from secondary and quaternary ones.

## 4. Abbreviations

ACL — Average Chain Length,  
APT — Attached Proton Test,  
COSY — CORrelated SpectroscopyY,  
DEPT — Distortionless Enhancement by Polarization Transfer,  
FACE — Fuels for Advanced Combustion Engines,  
FCA — Aromaticity Factor,  
GD — Gated Decoupling,  
HSQC — Heteronuclear Single Quantum Coherence,  
MON — Motor Octane Number,  
NMR — Nuclear Magnetic Resonance,  
PONA — Paraffins, Olefins, Naphthenes, and Aromatics,  
RON — Research Octane Number.

## 5. References

1. J.C.Edwards. *A Review of Applications of NMR Spectroscopy in the Petroleum Industry*. (New York: RAK, ASTM International, 2011). 638 p.
2. L.B.Krivdin. *Magn. Reson. Chem.*, **57**, 897 (2019); <https://doi.org/10.1002/mrc.4873>
3. L.B.Krivdin. *Magn. Reson. Chem.*, **58**, 5 (2020); <https://doi.org/10.1002/mrc.4896>
4. L.B.Krivdin. *Magn. Reson. Chem.*, **58**, 15 (2020); <https://doi.org/10.1002/mrc.4895>
5. L.B.Krivdin. *Magn. Reson. Chem.*, **60**, 733 (2022); <https://doi.org/10.1002/mrc.5260>
6. L.B.Krivdin. *Prog. NMR Spectrosc.*, **108**, 17 (2018); <https://doi.org/10.1016/j.pnmrs.2018.10.002>
7. L.B.Krivdin. *Prog. NMR Spectrosc.*, **112–113**, 103 (2019); <https://doi.org/10.7560/317587-103>
8. L.B.Krivdin. *Prog. NMR Spectrosc.*, **102–103**, 98 (2017); <https://doi.org/10.1016/j.pnmrs.2017.08.001>
9. V.A.Semenov, L.B.Krivdin. *Russ. Chem. Rev.*, **91** (5), RCR5027 (2022); <https://doi.org/10.1070/RCR5027>
10. L.B.Krivdin. *Molecules*, **26**, 2450 (2021); <https://doi.org/10.3390/molecules26092450>
11. A.G.A.Jameel, V.Van Oudenhoven, A.-H.Emwas, S.M.Sarathy. *Energy Fuels*, **32**, 6309 (2018); <https://doi.org/10.1021/acs.energyfuels.8b00556>
12. R.Meusinger. *Fuel*, **75**, 1235 (1996); [https://doi.org/10.1016/0016-2361\(96\)00053-1](https://doi.org/10.1016/0016-2361(96)00053-1)
13. J.Mühl, V.Srića. *Fuel*, **66**, 1146 (1987); [https://doi.org/10.1016/0016-2361\(87\)90314-0](https://doi.org/10.1016/0016-2361(87)90314-0)
14. J.Mühl, V.Srića, M.Jednačak. *Fuel*, **68**, 201 (1989); [https://doi.org/10.1016/0016-2361\(89\)90323-2](https://doi.org/10.1016/0016-2361(89)90323-2)
15. G.S.Kapur, A.P.Singh, A.S.Sarpal. *Fuel*, **79**, 1023 (2000); [https://doi.org/10.1016/S0016-2361\(99\)00238-0](https://doi.org/10.1016/S0016-2361(99)00238-0)
16. A.G.A.Jameel, N.Naser, A.-H.Emwas, S.Dooley, S.M.Sarathy. *Energy Fuels*, **30**, 9819 (2016); <https://doi.org/10.1021/acs.energyfuels.6b01690>
17. A.G.A.Jameel, N.Naser, G.Issayev, J.Touitou, M.K.Ghosh, A.-H.Emwas, A.Farooq, S.Dooley, S.M.Sarathy. *Combust. Flame*, **192**, 250 (2018); <https://doi.org/10.1016/j.combustflame.2018.01.036>
18. B.Basu, G.S.Kapur, A.S.Sarpal, R.Meusinger. *Energy Fuels*, **17**, 1570 (2003); <https://doi.org/10.1021/ef030083f>
19. O.L.Gulder, B.Glavincevski. *Ind. Eng. Chem. Prod. Res. Dev.*, **25**, 153 (1986); <https://doi.org/10.1021/i300022a005>
20. D.J.Cookson, B.E.Smith, R.R.M.Johnston. *Fuel*, **72**, 661 (1993); [https://doi.org/10.1016/0016-2361\(93\)90578-P](https://doi.org/10.1016/0016-2361(93)90578-P)
21. D.J.Cookson, P.Iliopoulos, B.E.Smith. *Fuel*, **74**, 70 (1995); [https://doi.org/10.1016/0016-2361\(94\)P4333-W](https://doi.org/10.1016/0016-2361(94)P4333-W)
22. V.Bansal, G.S.Kapur, A.S.Sarpal, V.Kagdiyal, S.K.Jain, S.P.Srivastava, A.K.Bhatnagar. *Energy Fuels*, **12**, 1223 (1998); <https://doi.org/10.1021/ef980052y>
23. D.J.Cookson, J.L.Latten, I.M.Shaw, B.E.Smith. *Fuel*, **64**, 509 (1985); [https://doi.org/10.1016/0016-2361\(85\)90086-9](https://doi.org/10.1016/0016-2361(85)90086-9)
24. D.J.Cookson, B.E.Smith. *Anal. Chem.*, **57**, 864 (1985); <https://doi.org/10.1021/ac00281a020>
25. D.J.Cookson, B.E.Smith. *Energy Fuels*, **4**, 152 (1990); <https://doi.org/10.1021/ef00020a004>
26. J.L.Burger, J.A.Widegren, T.M.Lovestead, T.J.Bruno. *Energy Fuels*, **29**, 4874 (2015); <https://doi.org/10.1021/acs.energyfuels.5b01035>
27. J.Mühl, V.Srića, B.Mimica, M.Tomaskovic. *Anal. Chem.*, **54**, 1871 (1982); <https://doi.org/10.1021/ac00248a049>
28. D.J.Cookson, B.E.Smith. *Energy Fuels*, **1**, 111 (1987); <https://doi.org/10.1021/ef00001a021>
29. R.B.Williams. *Spectrochim. Acta*, **14**, 24 (1959); [https://doi.org/10.1016/0371-1951\(59\)80215-0](https://doi.org/10.1016/0371-1951(59)80215-0)
30. A.J.Olaide, E.Olugbenga, D.Abimbola. *Int. J. Geosci.*, **11**, 145 (2020); <https://doi.org/10.4236/ijg.2020.114009>
31. G.A.Kalabin, L.V.Kanitskaya, D.F.Kushnarev. *Kolichestvennaya Spektroskopiya YaMR Prirodnogo Organicheskogo Syr'ya I Produktov ego Pererabotki. (Quantitative NMR Spectroscopy of Natural Organic Raw Materials and its Processing Products)*. (Moscow: Chemistry, 2000) 408 p.
32. D.F.Kushnarev, T.V.Afonina, G.A.Kalabin, R.N.Presnova, N.I.Bogdanova. *Petrol. Chem. U.S.S.R.*, **29**, 149 (1989); [https://doi.org/10.1016/0031-6458\(89\)90048-8](https://doi.org/10.1016/0031-6458(89)90048-8)
33. A.S.Sarpal, G.S.Kapur, S.Mukherjee, A.K.Tiwari. *Fuel*, **80**, 521 (2001); [https://doi.org/10.1016/S0016-2361\(00\)00123-X](https://doi.org/10.1016/S0016-2361(00)00123-X)
34. S.Mondal, K.Chattopadhyay, R.Kumar, J.Christopher, G.S.Kapur. *Energy Fuels*, **35**, 7883 (2021); <https://doi.org/10.1021/acs.energyfuels.1c00413>
35. B.K.Sharma, A.Adhvaryu, J.M.Perez, S.Z.Erhan. *Fuel Proc. Technol.*, **89**, 984 (2008); <https://doi.org/10.1016/j.fuproc.2008.04.001>
36. A.D.Ure, J.E.O'Brien, S.Dooley. *Energy Fuels*, **33**, 11741 (2019); <https://doi.org/10.1021/acs.energyfuels.9b01019>

37. S.Ok, T.K.Mal. *Energy Fuels*, **33**, 10391 (2019); <https://doi.org/10.1021/acs.energyfuels.9b02240>
38. A.B.Andrews, J.C.Edwards, A.E.Pomerantz, O.C.Mullins, D.Nordlund, K.Norinaga. *Energy Fuels*, **25**, 3068 (2011); <https://doi.org/10.1021/ef2003443>
39. T.Fergoug, Y.Bouhadda. *Fuel*, **115**, 521 (2014); <https://doi.org/10.1016/j.fuel.2013.07.055>
40. G.Gao, J.Cao, T.Xu, H.Zhang, Y.Zhang, K.Hu. *Fuel*, **271**, 117622 (2020); <https://doi.org/10.1016/j.fuel.2020.117622>
41. I.Z.Rakhmatullin, S.V.Efimov, V.V.Klochkov, M.A.Varfolomeev. In *Encyclopedia of Analytical Chemistry* (London: John Wiley and Sons, 2022); <https://doi.org/10.1002/9780470027318.a1828.pub2>
42. I.Z.Rakhmatullin, S.V.Efimov, M.G.Fazlyyyakhmatov, R.I.Galeev, V.V.Klochkov. In *NMR-Spectroscopy and NMR-Relaxometry* (London: John Wiley and Sons, 2023); <https://doi.org/10.1002/9781119871507.ch2-2>
43. I.Z.Rakhmatullin, S.V.Efimov, B.Ya.Margulis, V.V.Klochkov. *J. Petrol. Sci. Eng.*, **156**, 12 (2017); <https://doi.org/10.1016/j.petrol.2017.04.041>
44. I.Rakhmatullin, S.Efimov, M.Varfolomeev, V.Klochkov. *IOP Conf. Ser.: Earth Environ. Sci.*, **155**, 012014 (2018); <https://doi.org/10.1088/1755-1315/155/1/012014>
45. I.Z.Rakhmatullin, S.V.Efimov, V.A.Tyurin, A.A.Al-Muntaser, A.E.Klimovitskii, M.A.Varfolomeev, V.V.Klochkov. *J. Petrol. Sci. Eng.*, **168**, 256 (2018); <https://doi.org/10.1016/j.petrol.2018.05.011>
46. I.Rakhmatullin, S.Efimov, V.Tyurin, M.Gafurov, A.Al-Muntaser, M.Varfolomeev, V. Klochkov. *Processes*, **8**, 995 (2020); <https://doi.org/10.3390/pr8080995>
47. I.Z.Rakhmatullin, S.V.Efimov, E.I.Kondratyeva, L.M.González, K.R.Safiullin, M.A.Varfolomeev, A.V.Klochkov, V.V.Klochkov. *Petrol. Res.*, **7**, 495 (2022); <https://doi.org/10.1016/j.ptlrs.2022.01.001>
48. I.Z.Rakhmatullin, S.V.Efimov, A.V.Klochkov, O.I.Gnezdilov, M.A.Varfolomeev, V.V.Klochkov. *Petrol. Res.*, **7**, 269 (2022); <https://doi.org/10.1016/j.ptlrs.2021.10.001>